HYDRAULICS OPTIMIZATION OF FOAM DRILLING

A THESIS SUBMITTED TO
THE GRADUATE SCHOOL OF NATURAL AND APPLIED SCIENCES
OF
MIDDLE EAST TECHNICAL UNIVERSITY

BY

CEREN ÖZER

IN PARTIAL FULFILLMENT OF THE REQUIREMENTS
FOR
THE DEGREE OF MASTER OF SCIENCE
IN
PETROLEUM AND NATURAL GAS ENGINEERING

SEPTEMBER 2009

Approval of the thesis:

HYDRAULICS OPTIMIZATION OF FOAM DRILLING IN DRILLING OPERATIONS

submitted by **CEREN ÖZER** in partial fulfillment of the requirements for the degree of **Master of Science in Petroleum and Natural Gas Engineering Department, Middle East Technical University** by,

Prof. Dr. Canan Özgen _____
Dean, Graduate School of **Natural and Applied Sciences**

Prof. Dr. Mahmut Parlaktuna _____
Head of the Department, **Petroleum and Natural Gas Engineering**

Assoc. Prof. Dr. Evren Özbayoğlu _____
Supervisor, **Petroleum and Natural Gas Engineering Dept., METU**

Examining Committee Members:

Prof. Dr. Serhat Akın _____
Petroleum and Natural Gas Engineering Dept., METU

Assoc. Prof. Dr. Evren Özbayoğlu _____
Petroleum and Natural Gas Engineering Dept., METU

Prof. Dr. Mustafa Verşan Kök _____
Petroleum and Natural Gas Engineering Dept., METU

Prof. Dr. Tanju Mehmetoğlu _____
Petroleum and Natural Gas Engineering Dept., METU

Reha Özel, Ph.D. _____
Research Dept., TPAO

Date: 02-September-2009

I hereby that declare that all the information in this document has been obtained and presented in accordance with academic rules and conduct, I have fully cited and referenced all materials and results that are not original to this work.

Name, Last name : CEREN ÖZER

Signature :

ABSTRACT

HYDRAULICS OPTIMIZATION OF FOAM DRILLING IN DRILLING OPERATIONS

Özer, Ceren

M. Sc., Department of Petroleum and Natural Gas Engineering

Supervisor: Assoc. Prof. Dr. Evren Özbayoğlu

September 2009, 72 pages

In drilling, drilling fluid affects every single step of operation. If rig system is thought as the human body, drilling mud can be defined as the blood system of it. Drilling fluid carries the cuttings, cools the bit, it conditions the hole and so on. Some special kinds of drilling fluids are used for special purposes such as underbalanced drilling. Underbalanced drilling is generally used to prevent formation damage, lost circulation and to increase the penetration rate.Since 1980's foam is used as drilling fluid for underbalanced drilling purposes and there are some models for bit hydraulic optimizations.

In this study, mathematical model has been derived considering not the volumetric flow rate but the mass flow rate of the foams. Maximum hydraulic horse power at the bit is determined as a function of mass flow rate. Using this concept, optimum volumetric flow rates for liquid and gas phases as well as optimum nozzle size are determined.

Using this mathematical model, a computer program is developed for comparing the results with the existing data available in the literature. It accounts for the compressibility of foam and pressure losses inside the drill string, bit and annulus. Hole size, drill-string properties, formation temperature and pressure, maximum inlet pressure are used as input parameters. Program calculates static back pressure, pressure losses in the whole system, bottom hole foam properties such as quality and

velocity and optimum liquid and gas flow rates which are the key parameters of foam drilling optimization.

Results show that liquid and gas rates should be increased with increasing hole size and formation pressure. Increasing temperature gradient causes a minimal decrease on foam rate properties. In addition, pressure losses due to friction increases with increasing hole size and formation pressure. Decrease in formation temperature also decreases the foam quality. Changes in temperature gradient causes minimal changes on foam rate properties.

Comparisons of the proposed model with other models from the literature also gave good match. The optimization criteria and assumptions are differing from the existing models. As a result the comparison does not have to one to one match with the others. The results from this study may be used for optimization of flow rate of foam as drilling fluid based on mass flow.

Keywords: Drilling Fluid, Underbalanced Drilling, Foam, Hydraulic Optimization

ÖZ

SONDAJ OPERASYONLARI KÖPÜK SONDAJI HİDROLİK OPTİMİZASYONU

Özer, Ceren
Yüksek Lisans, Petrol ve Doğalgaz Mühendisliği Bölümü
Tez Yöneticisi: Doç. Dr. Evren Özbayoğlu

Eylül 2009, 72 sayfa

Sondaj sıvıları, sondaj operasyonlarının her aşamasını etkilerler. Eğer sondaj kulesi insan vücudu gibi düşünülürse, sondaj çamuru bu sistemin kanı olarak tanımlanabilir. Sondaj sıvısının; kesintileri taşımak, matkabı soğutmak, kuyuyu kondüsyona sokmak gibi pek çok önemli görevleri vardır. Farklı sondaj sıvıları, düşük basınçlı sondaj gibi özel durumlarda kullanılabilirler. Düşük basınçlı sondaj; formasyon kirlenmesi, kaçak durumlarını engellemek ve sondaj hızını arttırmak gerektiği zamanlarda tercih edilir. 1980'lerden beri köpük bu tür sondajlarda kullanılmakta olup, hidrolik optimizasyonu için bazı modeler bulunmaktadır.

Bu çalışmada, köpüğün, hacimsel akış debisi yerine, kütlesel akış debisi göz önünde bulundurularak matematiksel bir model geliştirildi. Matkapta oluşacak en yüksek hidrolik beygir gücüne, kütlesel akışa bağlı olarak ulaşıldı. Bu şekilde, gaz ve sıvı fazlar için optimum hacimsel akış debileri ve nozzle ölçüleri hesaplandı.

Bu matematiksel modele dayalı bir bilgisayar programı yazılarak, literatürdeki veriler ile karşılaştırıldı. Bu program köpüğün sıkıştırılabilirliğini, sondaj dizisi içindeki, matkapdaki ve açık kuyudaki basınç kayıplarını göz önünde bulundurmaktadır. Açık kuyu çapı, sondaj dizisi özellikleri, formasyon basınç ve sıcaklıkları ve maksimum giriş basınçları girdi olarak kullanılmaktadır. Bu verilere dayanarak, statik ters basınç, sistemdeki basınç kayıpları, kalite ve hız gibi kuyu dibi köpük özellikleri, optimum sıvı ve gaz akış debileri çıktı olarak hesaplamaktadır.

Sonuçlara göre artan kuyu çapı ve formasyon basıncıyla sıvı ve gaz debileri de arttırılmalıdır. Ayrıca, kuyu çapı ve formasyon basıncı arttıkça sürtünmeden kaynaklanan basınç kayıplarının da arttığı görülmüştür. Formasyon sıcaklığındaki düşüşün köpük kalitesininde azalmasına sebep olacağı görülmüştür. Sıcaklık değişimleri köpük debisinde ise önemli bir değişiklik yaratmamaktadır.

Önerilen model ve literatürdeki benzer çalışmaların karşılaştırılması uyumlu sonuçlar vermiştir. Ancak optimizasyon kriterleri ve varsayımlar diğer modellerden farklı olduğu için, sonuçların bire bir uyumu söz konusu değldir. Bu çalışmanın sonuçları, sondaj sıvısı olan köpüğün kütle akışına bağlı olarak optimizasyonunda kullanılabilir.

Anahtar Kelimeler: Sondaj Sıvısı, Düşük Basıçlı Sondaj, Köpük, Hidrolik Optimizasyon

ACKNOWLEDGEMENTS

First and foremost, I would like to express my deepest gratitude to my advisor Assoc. Prof. Dr. M. Evren Özbayoğlu for his support through all stages of this study. His comments and guidance has been inspirational for me and for the work presented.

I also wish to express my warm and sincere thanks to my committee members Prof. Dr. Serhat Akın, Prof. Dr. Mustafa Verşan Kök, Prof. Dr. Tanju Mehmetoğlu and Reha Özel for all their support through my career. They all have influenced me to become a better engineer.

I would like to extend my thanks to my mother, my sister, my father and my grandfather Mümtaz Özer.

I also want to express my special thanks to Emre Doruk Tanyel for his help with this study.

Last, I would like to thank to TPAO Drilling Department for giving me support and the opportunity to chase one of my career goals of having an advanced engineering education.

TABLE OF CONTENTS

LIST OF TABLES

TABLES

LIST OF FIGURES

FIGURES

NOMENCLATURE

GLR	Gas to Liquid Ratio, dimensionless
Γ	Foam quality index, dimensionless
V_g	Gas Volume, scf
V_l	Liquid Volume, gallons
V_f	Formation Fluid Influx Volume, gpm
ρ_g	Density of the gas phase, lb/ft^3
ρ_l	Density of the liquid phase, lb/ft^3
Q_g	Gas injection rate, scfm
Q_l	Liquid injection rate, gpm
Q_f	Formation influx rate, gpm
A	Flow path cross sectional area, in^2
$\dot{m}$	Mass flow rate, lb/min
μ_F	Foam viscosity, lb/ft-sec
μ_u	Base liquid viscosity, lb/ft-sec
μ_o	Bingham viscosity, lb/ft-sec
LVF	Liquid Volume Fraction, dimensionless
μ_e	Effective viscosity, lb/ft-sec
$\dot{\gamma}$	Shear rate, sec^{-1}
n	Power-law flow behavior index
d_H	Hydraulic diameter, in
f_m	Moody friction factor, dimensionless
f_f	Fanning friction factor, dimensionless
N_{RE}	Reynolds number, dimensionless
N_{REM}	Modified Reynolds number, dimensionless
L	Length of pipe, ft
d	Inner diameter of pipe, in
g	Acceleration due to gravity, ft/s^2
h_f	Head loss, psi

P_{bh}	Bottom hole pressure, psi
P_{up}	Nozzle's upstream pressure, psi
v_n	Nozzle velocity, ft/sec
v_{up}	Velocity upstream of the nozzle,ft/sec
m_g	Mass of gas, lb_m
m_l	Mass of liquid, lb_m
M	Molecular weight of gas, lb_m
ΔP_b	Pressure drop at the bit, psi
$\bar{z}$	Mean gas deviation factor, dimensionless
R	Universal gas constant, ft lb/slug ^oR
T	Absolute temperature, ^oR
g_c	Conversion constant, ft/s^2
HP_{bit}	Hydraulic horsepower at the bit, HP
Q	Flow rate, scfm
HP_p	Total power generated at the pump, HP
$HP_{\Delta P_b}$	Total of power lost at the bit, HP
$HP_{\Delta P_f}$	Power lost in the circulating system due to friction, HP
$HP_{\Delta P_{fpipe}}$	Power lost in the pipe, HP
$HP_{\Delta P_{fann}}$	Power lost in the annulus, HP
A	Flow Area, in^2
V	Velocity, ft/sec
D	Diameter, in

CHAPTER 1

INTRODUCTION

Oil companies began drilling wells with air in the late 1940s with the motivations to increase drilling penetration rates through hard formations and to overcome severe lost circulation problems. Increased rates of penetration as a result of reduced differential pressure at the bottomhole were the most important benefit of the early applications of underbalanced drilling. This effect can be seen in **Figure 1** from the works of Moffitt[1]. The beneficial effects of reduced hydrostatic pressure with regard to increased drilling rates occurred at all bit weights.

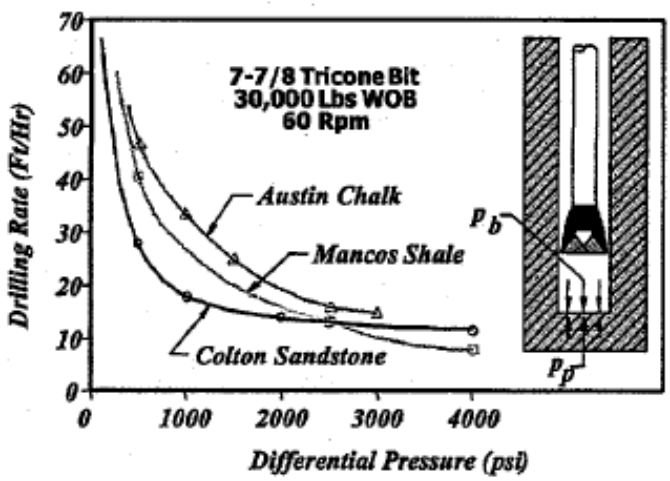

Figure 1 Differential Pressure vs. Drilling Rate (Moffitt, 1991)

Other benefits of air drilling included reduced formation damage, reduced lost circulation and fewer problems with differential sticking. Many tight gas reservoirs, where tight (low-permeability) formations are more susceptible to formation damage from invasion of conventional drilling fluids, became ideal candidates for underbalanced drilling. During the following decades, the variety of underbalanced drilling fluids was expanded to include mist, foam, and aerated fluids. A commonly

used picture for describing the flow regimes from the works of Lorenz[2] is shown in **Figure 2**.

Foam was first used as a workover fluid in 1969 and as a drilling fluid in the late 1980s. Foams have viscosity values greater than both constituents, at a constant shear rate which makes them very good for efficient cuttings transport.

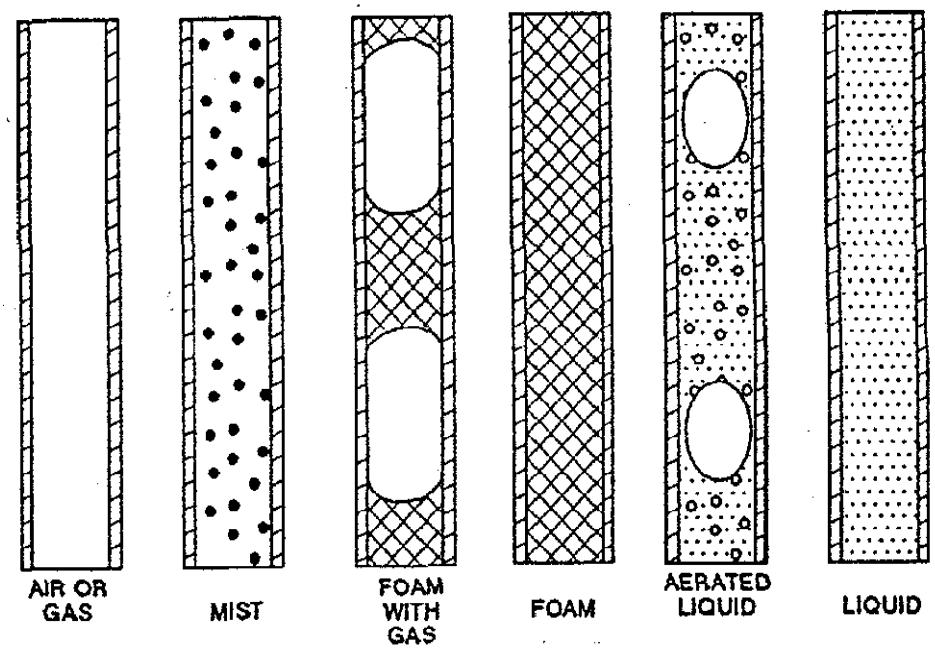

Figure 2 Types of Underbalanced Drilling Fluid Defined by Flow Regimes (Lorenz, 1980)

However, the introduction of these two-phase fluids was accompanied by significantly increased difficulty in predicting fluid flow parameters with these compressible fluids.

There is no universally accepted model for defining the complex behavior of these fluids at the moment. On the other hand, even though the idea is working, in order to be able to have control over this concept the understanding must be clear. Therefore time and effort should be given and studies must be conducted on this concept.

CHAPTER 2

LITERATURE REVIEW

2.1. FOAM DRILLING

Foam is two phase liquid-gas dispersion with the liquid as the continuous phase and the gas as the dispersed phase. The incompressible component is usually fresh water and a surfactant foaming agent. The compressible component is generally air. In some cases, natural gas, CO_2, nitrogen can be used. For drilling applications, some other additives such as viscosifiers, lubricants, corrosion inhibitors and stabilizers may also be used depending on the hole conditions.

Foams can be classified as, “Stiff Foam”, and “Stable Foam” for discussion purposes.

2.1.1. Stiff Foam

Stiff foam was first introduced by U.S Atomic Energy Commission for drilling large diameter holes in poorly consolidated formations[3]. Thus, stiff foam is a low density drilling fluid, used to drill unconsolidated formations in which some hole stabilizing materials can be used. For adequate hole cleaning, annular velocity can be from 100 to 200 ft\min.

Compared with the other types of pneumatic drilling fluids, the compressor requirements are much less. While preparing stiff foam, firstly polymers are premixed with water. Than in the foam tank, foaming agent is added by mixing slowly. After that it is injected to the air stream. The air-mud ratio varies 100:1 to 300:1. In order to prevent air breakout in the annulus the foam is similar to the consistency of aerosol shaving cream. Stiff foam cannot be re-circulated and must be

discarded at the surface. The disadvantage of stiff foam is being ineffective with salty water and oil. The composition of stiff foam is given in **Table 1**.

Table 1 Composition of Stiff Foam

ADDITIVE	lb\bbl	Vol. %	Function
Prehydrated Bentonite		-	Builds Foam Structure
Carboximethylcellulose (CMC)	0.5	-	Foam Stabilizer Drying Agent
Guar Gum	0.2-0.5	-	Foam Stabilizer
Soda Ash	0.5-0.1	-	Calcium Treating Agent
Caustic Soda/Caustic Potash	0.55-0.5	-	Corrosion Protection
Foaming Agent	-	1%	Stabilizes Air in Liquid
Potassium Chloride	-	3-5%	Shale Stabilizer
Filming Amine	-	0.50%	Corrosion Protection

2.1.2. Stable Foam

Stable foam differs with stiff foam with its preparing method. Stable foam is prepared in a surface foam generating unit **(Figure 3)**. The simple equipment consists of an air compressor, a blending tank, a detergent solution pump, a foam generator and an injection manifold.

Generally, stable foam consists of water, detergent and gas. Sometimes it may include viscosifiers, salts or corrosion inhibitors. Again as stiff foam it is circulated only once.

Selection of mixing components should be carefully controlled to prepare foam with density as low as 2 lbs/ ft^3. High lifting capacities result when annular velocities equal or exceed 300 feet\minute. Besides, depending on the down hole conditions, stable foam should have gas liquid volume ratio of 3 to 50 ft^3/gal in general. General additives of stable foam and their functions are shown in **Table 2**.

Table 2 Composition of Stable Foam

ADDITIVE	lb\bbl	Vol. %	Function
Prehydrated Bentonite	10 - 15	-	Foam Stabilizer
Polyanionic Cellulose	0.5	-	Filtration Agent
Sodium Polyacrlate	1	-	Drying Agent
Foaming Surfactant	-	1%	Filtration Agent
Potassium Chloride	-	3-5%	Foaming Agent
XC Polymer	0.25-1	-	Borehole Stabilizer
Filming Amine	-	0.50%	Foam Stabilizer
Lime	0.25-0.5	-	Corrosion Protection

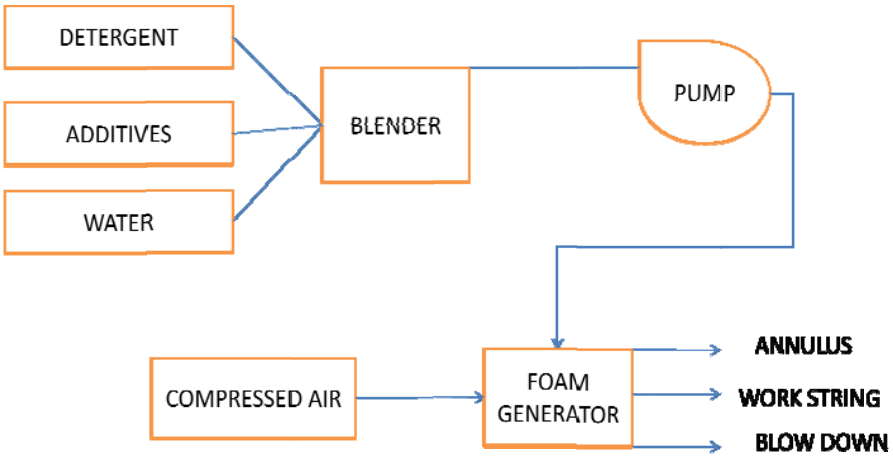

Figure 3 Stable Foam Mixing System

2.1.3. Benefits of Foam for Underbalanced Drilling:

Foams were introduced to the oil and gas drilling industry as a drilling fluid capable of overcoming problems encountered with air or mist as it had improved lifting capacity over them.

Influx is an important problem when air is the drilling fluid. Even small volume of influx may trigger the cuttings to stick together and thus hinder the cleaning. To prevent this, water may be added to wet the cuttings in order to prevent packing as done in mist drilling. However, when the influx rate is large, the hole cleaning may even stop and the circulation might be lost. Typical solution with air or mist drilling will be to fill up the well with mud, kill the well, and continue to drill. But this would also decrease the rate of penetration and also would cause an overbalanced condition that would contaminate the formation.

Alternatively, foams can handle large influx volumes out of the wellbore, especially if the influx fluid is water. If the influx is hydrocarbon or saltwater then special care must be given to the chemicals used in the design of the foam to prevent its collapse.

Foams also have the advantage of increased cuttings carrying capacity, this can be seen in **Figure 4** from the works of Beyer et al[4]. As the foam quality increases the lifting force increases. The maximum lifting force is achieved between 0.95 to 0.98 foam qualities. As foam becomes wetter, its viscosity and ability to carry cuttings decrease. Conversely, when the fluid crosses into a gas continuous phase it can lift the cuttings well but its ability to hold the cuttings in suspension disappears.

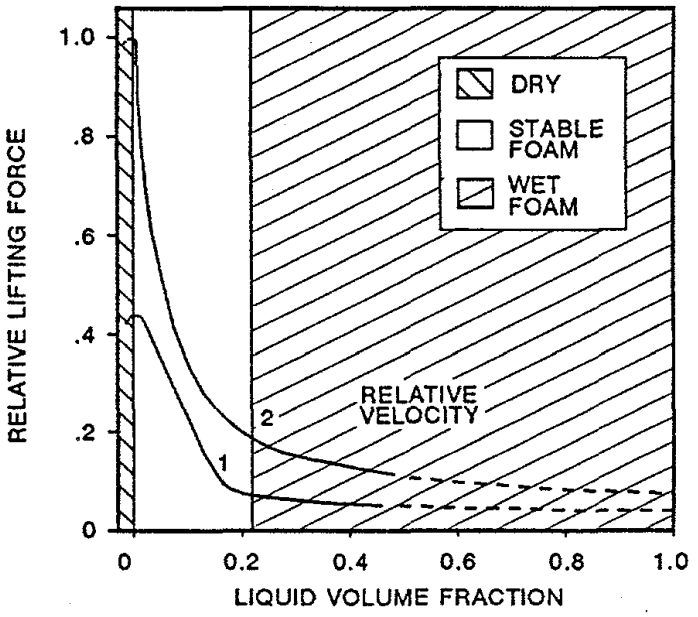

Figure 4 Foam Lifting Capacity (Beyer et al., 1972)

2.2. FOAM RHEOLOGY AND BEHAVIOR

Sibree[5] was the first to discuss the concept of foam rheology. He found that the apparent viscosity of foam was higher than the viscosities of each of its constituents. He also proposed that behavior of foam was Newtonian below critical shear stress value and plug like above that.

Raza and Mardsen[6] performed experimental studies of flow of foams through pyrex tubes and concluded that foams having qualities in the range of 70% - 96% behaved as pseudoplastic fluids. They further stated that laminar flow was observed at lower flow rates; plug like behavior was observed at high flow rates and viscosity was dependent on the foam quality and pipe diameter. Their results did not consider slippage at the tube wall and the compressibility of the foam.

David and Mardsen[7] in their theoretical and experimental studies using capillary tube viscometer consisting of various diameters also integrated the slippage at the wall and compressibility of the foam. They concluded that, when the apparent viscosity was corrected for both slippage and compressibility, it is independent of foam

quality. They also observed that the slip coefficient increased with the shear stress and apparent viscosity was dependent on the tube diameter.

Beyer, et al.[4] used experimental and pilot-scale data with a finite difference approach for modeling the foam flow in vertical pipes and annuli. Their model was valid for foam qualities over 0.75 and took into account slippage at the pipe wall. They pointed out that the liquid volume fraction was the principle independent variable affecting the foam flow behavior.

Blauer, et al.[8] proposed to calculate the Reynolds number and the Fanning friction factor for foams using the effective viscosity, actual density, average velocity and the pipe diameter. They found that for foams, the relation of the Reynolds number and Fanning friction factor was the same as that of a single-phase fluid. They concluded that foam behaves like a single phase Bingham plastic fluid and foam plastic viscosity and yield strength can be determined as a function of foam quality.

Lord[9] presented an equation of state based on real gas law and mass balance conservation. He assumed an average friction factor for the whole system which needed to be determined very carefully for the model to produce good results. The model then by numerical solution of mechanical energy balance equation for compressible fluid flow accurately predicted downhole pressures when proppant-loaded foam was pumped down a well.

Sanghani[10] performed experiments using a concentric annular viscometer to simulate wellbore conditions. He found that Power-Law model was statistically better than the Bingham model to correlate the data. Based on the experimental data he also proposed correlation of pseudoplastic parameters as a function of foam quality.

Okpobiri and Ikoku[11] presented a model for predicting volumetric requirements for foam drilling. The model accounted for the compressibility of foam, the frictional losses caused by the cuttings and the pressure drop at the bit, but neglected the pressure losses of foam due to friction and the change in elevation. They concluded

that the volumetric requirements increase with the hole size. They also stated that in order to clean the cuttings effectively a minimum of 55% bottomhole foam quality was required and this was only possible by application of annular backpressures greater than the atmospheric pressure.

Sanghani and Ikoku[12], based on experimental data, concluded that foam behavior is pseudoplastic and the effective velocity decreases with increasing shear rate for a defined foam quality. They also stated that, as foam has low density and high viscosity, if the bottomhole quality is over 55% foam drilling operations can be carried out in the laminar flow region.

Reidenbach, et al.[13] performed experiments with foams using N_2 as the internal phase. They proposed models describing the laminar flow of foam through pipes. Substitution of CO_2 for N_2 as the internal phase also presented similar laminar rheology. They used a modified scale-up relationship to describe turbulent flow of compressible foam.

Spoerker, et al.[14] modified Lord[9]'s pressure drop equation and proposed a new two-phase downward flow where the gas compressibility factor was not constant. They solved the differential mechanical energy balance equation presenting a clear expression for pressure loss of foam flow. In the case of incompressible fluids their equation reduced to the Fanning pressure drop equation.

Guo, et al.[15] presented an iterative method to estimate the hydrostatic head and the frictional losses along the annulus when foam is used as the drilling fluid. Assuming that foam is a Power-Law fluid, they calculated pressures through use of the foam density stating that the frictional and hydrostatic pressure components influence each other through the pressure dependent fluid density.

Liu and Meldy[16] used an improved version of Lord[9]'s pressure drop equation and Spoerker[14]'s method to calculate the Fanning friction factors along the path of flow. They proposed a model that used injection pressure, backpressure and injection rates

to numerically determine the foam characteristics as a function of depth and cuttings concentration using an equation of state for real gas and a mechanical energy balance.

Gardiner, et al.[17] used experimental data from a Poiseuille-flow rheometer. They derived a master equation describing expansion ratios and pressures encountered during pumping of polyhedral foams. The result demonstrated an equalized Power-Law relationship that can be used to give velocity profiles for laminar flow of foams in tubes.

Argillier, et al.[18] performed rheological experiments using a closed-loop flow system. They considered physico-chemical properties of foam and examined the effects of presence of hydrocarbons and salt on foam stability. They used the volume equalized approach to calculate the frictional pressure losses.

Özbayoğlu, et al.[19] conducted a rheological study for foam comparing six different rheological models with experimental data. They pointed out that the wall slip effect should not be considered negligible in order to establish flow behavior of foam in pipes. Their experiments indicated that there was no single rheological model to describe foam flow at all qualities and that foam rheology can be characterized as a Power-Law fluid at lower qualities and Bingham Plastic gives better fits for qualities higher than 0.90.

Guo, et al.[20] considering foam behavior to be Power-Law, presented a closed form analytical hydraulic model for predicting foam hydraulics. Their model accounted for frictional and hydraulic pressure components in vertical and inclined wellbores. They compared the results from their model with field data from two wells drilled using stable foam. The difference from the results of their model and the actual field data was maximum 9.2%.

Sun[21] used Guo et al.[20]'s foam hydraulics model to derive Equivalent Circulating Density, Equivalent Mud Weight, minimum backpressure and depth limit curves for

stable foam drilling with different Gas to Liquid Ratios. He concluded that GLR was the dominating factor influencing the Equivalent Circulating Density, Equivalent Mud Weight and the depth limit with stable foam drilling.

Eren[22] performed experimental studies on the effects of the bubble size and texture of foam on the foam behavior. He concluded that the accuracy of the estimations for pressure losses was increased when the bubble size and the texture of foam were taken into account and the foam quality increases as the foam circularity decreases and the bubble size increases.

Kuru, et al.[23] conducted studies in efforts to optimize the drilling hydraulics of foam drilling. They stated that while maintaining a minimum bottomhole temperature, the maximum drilling rates and effective cuttings transport could be achieved by controlling the backpressure, foam quality, gas/liquid flow rates, and bit-nozzle sizes.

Doğan et al.[24] used the general energy equation in their work for estimating the pressure drop at the bit using gasified fluids having critical and sub-critical flow regimes. They compared their findings with commercial programs available in the industry to see that the maximum difference they encountered was 9% and concluded that this alternative approach gave good results.

CHAPTER 3

STATEMENT OF THE PROBLEM

As the search for oil continues to investigate harder targets, drilling operations are becoming much expensive and even more complicated. Foam drilling may be considered as one of the relatively newer drilling techniques that needs a better understanding because of its increasingly complex hydraulics calculations.

During the literature survey, it is seen that there are numerous models for the hydraulics of single phase fluids based on either field data or based on theory. Most of them neglected the pressure losses due to friction especially for liquid phase. In this study it is aimed to consider all frictional losses in the circulating system. Also hydraulics calculations of foam differ from hydraulics of 100% liquids since liquids can be assumed as incompressible. 100% gas is still easier to model than foam since even though it is compressible, it is also one continuous phase. The hydraulics of foam and mist can probably be considered the hardest to model since these fluids both are two-phase and compressible. The existing models do not take compressibility of gas into account. The main goal of this research is using mass flow rate instead of volume flow rate and prevent miscalculations resulting from volume changes.

Drilling wells using foam has been a successful practice for many field applications but there is a lack of understanding what is really happening in the wellbore. Early calculations of foam hydraulics were based on using nomography and charts. However even with the rapid development in the technology and the availability computers there is still not an easy answer to the foam hydraulics.

Understanding the drilling fluids and drilling approach can help in assessment of the potential drilling-induced formation damage issues. This in turn will assist in

choosing solutions appropriate for a given formation/well. For many reservoirs, such as fractured, vugular formations and tight gas reservoirs, using foam as drilling fluid can be the best practice. However, when foam is selected as the drilling fluid one must pay attention, since there is the potential for severe formation damage if it is not properly executed.

There are simulators available in the drilling industry for steady state and the transient flow foam drilling hydraulics calculations but they present conflicting results. They present different solutions mainly because of the assumptions that they make during the development of the mathematical and the rheological models. Therefore it can be concluded that, in order to have a thorough understanding of the complex nature of the hydraulics of foam drilling, there is still work to be done.

A different approach than previous studies may be to form the mathematical model based on the mass flow rate of the foams instead of the volumetric flow rate. In this study, the maximum hydraulic horse power at the bit is determined as a function of mass flow rate. Based on this, optimum volumetric flow rates for liquid and gas phases as well as optimum nozzle size are determined. The results can be used for field applications and improve the penetration rate and effectiveness of foam for a drilling operation. Also, it is a new approach to foam hydraulic optimization, it can help delivering a less damaged formation due to usage of foam.

CHAPTER 4

METHOD OF SOLUTION

4.1. THEORY

4.1.1 Foam Quality

Foam quality is the ratio of the volume of gas phase to gas/liquid phase[3]. The foam quality index is denoted by Γ and can be defined as;

$$\Gamma = \frac{V_g}{V_g + V_l + V_f} \quad \text{(Eq. 4.1)}$$

where;

V_g = Gas Volume
V_l = Liquid Volume
V_f = Formation Fluid Influx Volume

Foam is compressible just like any other multi-phase fluid. Thus, the quality of foam is a function of the pressure exerted on it. Increased pressure decreases the volume of the gas phase which decreases the quality. Therefore, foam quality at the bottomhole conditions may be very different from the quality at surface conditions. Foam is Newtonian for qualities below 0.55 and Non-Newtonian above. When the quality is over 0.97 the gaseous phase becomes unstable and foam turns into mist.

4.1.2 Foam Desity

The density of foam can be expressed as;

$$\rho_f = \Gamma\rho_g + (1-\Gamma)\rho_l \quad \text{(Eq. 4.2)}$$

where;

ρ_g = density of the gas phase

ρ_l = density of the liquid phase

4.1.3 Foam Velocity

The foam velocity can be calculated as;

$$v_f = \frac{Q_g + Q_l + Q_{fi}}{A} \quad \text{(Eq. 4.3)}$$

where;

Q_g = Gas injection rate

Q_l = Liquid injection rate

Q_{fi} = Formation influx rate

A = Flow path cross sectional area

Assuming zero formation influx, the total flow rate can be calculated as;

$$Q_t = \frac{\dot{m}}{\rho_f} \quad \text{(Eq. 4.4)}$$

where;

$\dot{m}$ = mass flow rate

4.1.4 Foam Viscosity

Einstein[25] was the first to propose a model for a dispersed system. His approach was to consider foam similar to suspension of solids in liquid and use an energy balance. For foam qualities from 0 to 0.45 his equation relating viscosity to foam quality given by;

$$\mu_F = \mu_u(1 + 2.5\Gamma) \quad \text{(Eq. 4.5)}$$

where;
μ_F = Foam viscosity
μ_u = Base liquid viscosity

Hatschek[26, 27] also developed similar models. For the region of 0 to 0.74 quality, his approach was to use Stoke's law for a slowly falling ball. His resulting equation was;

$$\mu_F = \mu_u(1 + 4.5\Gamma) \quad \text{(Eq. 4.6)}$$

For qualities from 0.74 to 1.00 he presented another equation based on conservation of energy during interference, deformation, and packed bubbles within a flow boundary given by;

$$\mu_F = \mu_u \left(\frac{1}{1-\Gamma^{\frac{1}{3}}}\right) \quad \text{(Eq. 4.7)}$$

Mithchell[28] based his model on Rabinowitsch's theory and proposed two empirically derived equations for foam viscosity (**Figure 5**). The model he proposed for qualities from 0 to 0.54 was;

$$\mu_F = \mu_u(1 + 3.6\Gamma) \quad \text{(Eq. 4.8)}$$

The equation he proposed for qualities ranging from 0.54 to 0.97 was;

$$\mu_F = \mu_u \left(\frac{1}{1-\Gamma^{0.49}}\right)$$ ..... (Eq. 4.9)

Beyer, et al.[4], based on their field scale experiments, concluded that foam velocity had a slip component and a fluidity component. Based on the liquid volume fraction (1-Γ) they calculated viscosity as;

For 0.02 < LVF < 0.10;

$$\mu_o = \frac{1}{(7200LVF+267)}$$ ..... (Eq. 4.10)

For 0.10 < LVF <0.25;

$$\mu_o = \frac{1}{(2533LVF+733)}$$ ..... (Eq. 4.11)

where;

μ_o = Bingham viscosity

LVF = Liquid Volume Fraction

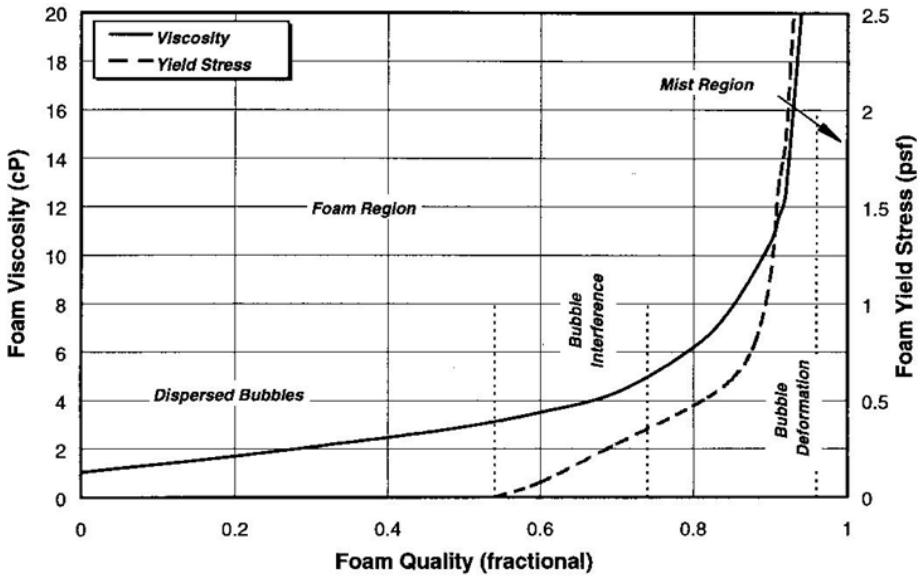

Figure 5 Viscosity and Yield Point of Foam as Functions of Foam Quality (Mitchell, 1971)

Sanghani and Ikoku[12], conducted experiments that closely simulated actual hole conditions. They presented empirical results (**Table 3**) for the relation of the effective viscosity (μ_e) to foam quality for different values of shear rate given by;

$$\dot{\gamma} = \left(\frac{2n+1}{3n}\right)\left(\frac{12v_f}{d_H}\right) \quad \text{(Eq. 4.12)}$$

where;

$\dot{\gamma}$ = Shear rate

n = Power-law flow behavior index

d_H = hydraulic diameter

Table 3 Effective Viscosity, Foam Quality Relationship for Different Values of Shear Rate (Sanghani and Ikoku[12], 1983)

	Effective Viscosity (cp)									
Γ	γ (s^{-1}) =100	γ (s^{-1}) = 200	γ (s^{-1}) = 300	γ (s^{-1}) = 400	γ (s^{-1}) = 500	γ (s^{-1}) = 600	γ (s^{-1}) = 700	γ (s^{-1}) = 800	γ (s^{-1}) = 900	γ.(s^{-1}) =1000
0.998 - 1	52.4	28.2	19.5	15.1	12.3	10.5	9.1	8.1	7.3	6.6
0.97	289.4	181.4	138.0	113.7	97.8	86.5	78.0	71.2	65.8	61.3
0.95	341.7	208.9	156.5	127.7	109.0	95.8	85.8	78.1	71.8	66.6
0.92	530.7	302.1	217.3	172.0	143.4	123.7	109.1	97.9	89.0	81.6
0.90	492.9	283.1	204.7	162.6	136.0	117.5	103.9	93.4	85.0	78.1
0.85	437.7	253.2	183.8	146.4	122.8	106.3	94.1	84.7	77.2	71.0
0.80	349.4	209.2	155.0	125.3	106.2	92.8	82.8	75.0	68.7	63.6
0.75	307.6	189.3	142.6	116.6	99.7	87.8	78.8	71.7	66.1	61.4
0.70	292.7	180.2	135.6	110.9	94.9	83.5	75.0	68.3	62.9	58.4
0.67	284.1	173.7	130.3	106.2	90.6	79.6	71.4	65.0	60.0	55.4

4.1.5 Friction Factor

Two different friction factors are defined in the literature. The Moody friction factor, which is also called the Darcy Weisbach friction factor, and the Fanning friction factor. They are both functions of Reynolds number but the former is 4 times bigger than the latter. The equation for the Moody friction factor is;

$$f_m = \frac{64}{N_{Re}} \quad \text{(Eq. 4.13)}$$

and the equation for the Fanning friction factor is;

$$f_f = \frac{16}{N_{Re}} \quad \text{(Eq. 4.14)}$$

For which the Reynolds number can be calculated as;

$$N_{Re} = \frac{v_f d_H \rho_f}{\mu_e} \quad \text{(Eq. 4.15)}$$

4.1.6 Foam Head Loss

Calculation of the head loss needs special attention because there are two different formulas for the two different friction factors. The equation for head loss using the Moody friction factor is;

$$h_f = f_m \left(\frac{L}{d}\right)\left(\frac{v^2}{2g}\right) \quad \text{(Eq. 4.16)}$$

where;
L = Length of pipe
d = Inner diameter of pipe
g = Acceleration due to gravity

Similarly, the head loss using the Fanning friction factor is;

$$h_f = f_f \left(\frac{L}{d_H}\right)\left(\frac{v^2}{2g}\right) \quad \text{(Eq. 4.17)}$$

Although they look very similar there is a difference occurring because of the diameter term that is used. When using the Fanning friction factor, the hydraulic radius will be used whereas when using the Moody friction factor, the pipe diameter will be used.

For a round pipe with full flow the hydraulic radius is equal to ¼ of the pipe diameter. This difference will account for the 4 times difference occuring between the friction factors.

4.1.7 Pressure Drop Across Bit Nozzles

Nozzles are small orifices installed on the bit which cause the interchange of kinetic and internal energy of a fluid during flow due to a change in the cross sectional area of the path of flow. Therefore, significant pressure drops occur across the nozzle. A common drawing of the flow through a nozzle by Azar[29] is shown in **Figure 6**.

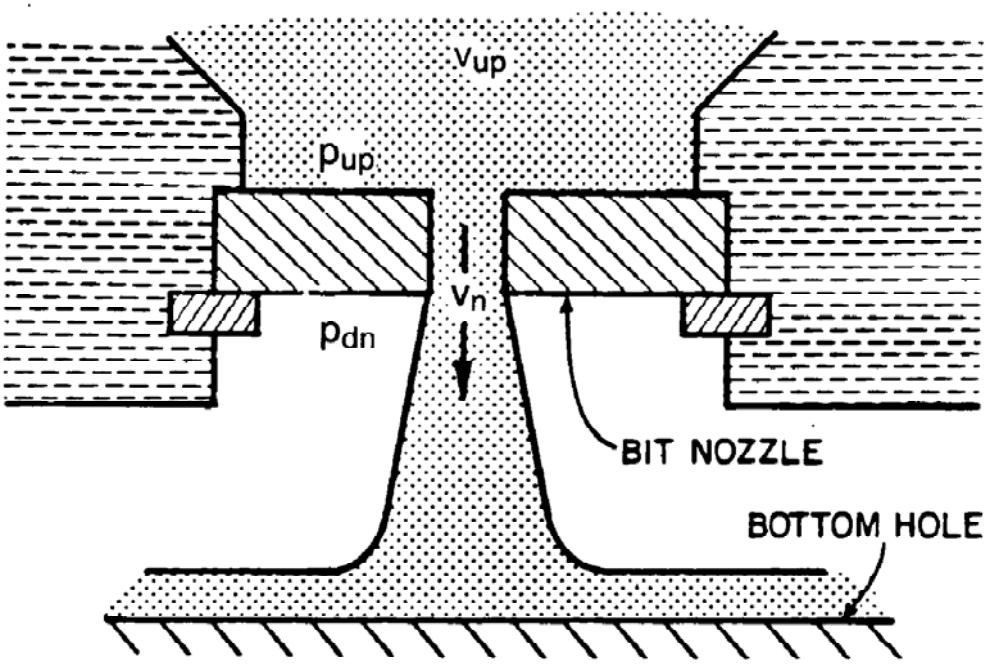

Figure 6 Flow Through a Bit Nozzle (Azar, 1982)

There is no single model to define the flow of two phase fluids across a nozzle mainly because the formulation differs based on the gas fraction of gas and the flow regime. The model developed by Okpobiri and Ikoku[11] works good for foam provided that the flow is steady-state and isentropic. The equations they presented for the pressure drop at the bit was;

$$\Delta P_b = \frac{\bar{A}}{B}\left[ln\frac{P_{bh}}{P_{up}} + E\left(v_n^2 - v_{up}^2\right)\right] \quad \text{(Eq. 4.18)}$$

$$\bar{A} = \frac{m_g \bar{z} R T}{M\left(m_g + m_l\right)}$$

$$B = \frac{m_l}{\rho_l\left(m_g + m_l\right)}$$

$$E = \frac{1}{2\bar{A}g_c}$$

where;

P_{bh} = Bottomhole pressure

P_{up} = Nozzle's upstream pressure

v_n = nozzle velocity

v_{up} = Velocity upstream of the nozzle

m_g = Mass of gas

m_l = Mass of liquid

M = Molecular weight of gas

$\bar{z}$ = Mean gas deviation factor

R = Universal gas constant

T = Absolute temperature

g_c = Conversion constant

However, in practice, generally the upstream velocity is assumed to be negligible since the nozzle velocity is much larger than the upstream velocity. Therefore the equation for the pressure drop at the bit simplifies to;

$$\Delta P_b = \frac{\bar{A}}{B}\left[ln\frac{P_{bh}}{P_{up}} + Ev_n^2\right] \quad \text{(Eq. 4.19)}$$

4.1.8 Bit Hydraulic Horsepower

Hydraulic horsepower is a measure of the energy per unit of time that is being expended across the bit nozzles. A common and well accepted approach for optimum bottom hole cleaning is by optimizing the hydraulic horsepower at the bit. The hydraulic horsepower at the bit can be calculated as;

$$HP_{bit} = \frac{\Delta P_b Q}{1714} \quad \text{(Eq. 4.20)}$$

When the optimum flow rate is calculated, it is possible to define the optimum flow area and the optimum nozzle sizes accordingly.

4.2. MATHEMATICAL MODEL

The total power generated at the pump will be equal to the total of power lost at the bit and the power lost in the circulating system due to friction.

$$HP_p = HP_{\Delta P_b} + HP_{\Delta P_f} \quad \text{(Eq. 4.21)}$$

Aim: $HP_{\Delta P_b} \rightarrow MAX$

$HP = Q \times P$

The flow rate can be considered in terms of mass rate as;

$$Q = \frac{\dot{m}}{\rho_{|P,T}} \quad \text{(Eq. 4.22)}$$

Assuming that the main part of the foam density is coming from the liquid, the equation for the foam density reduces to;

$$\rho = \rho_L(1 - \Gamma) \quad \text{(Eq. 4.23)}$$

The power lost in the circulating system due to friction may be written as the sum of the power lost in the pipe and the power lost in the annulus;

$$HP_{\Delta P_f} = HP_{\Delta P_{fpipe}} + HP_{\Delta P_{fann}} \quad \text{(Eq. 4.24)}$$

Therefore, rearranging for the power lost at the bit and substituting mass rate and density yields to;

$$HP_{\Delta b} = HP_p - HP_{\Delta P_f} \quad \text{(Eq. 4.25)}$$

$$HP_{\Delta P_b} = \left[\frac{\dot{m}}{\rho_L\,(1 - \Gamma_{@P_p})}\,P_p\right] - \left[\frac{\dot{m}}{\rho_L\,(1 - \Gamma_{@pipe})}\,\Delta P_{f_{pipe}}\right] - \left[\frac{\dot{m}}{\rho_L\,(1 - \Gamma_{@ann})}\,P_{f_{ann}}\right]$$

$$\Delta P_f = c\,\dot{m}^{\xi}$$

$$HP_{\Delta P_b} = \left[\frac{\dot{m}}{\rho_L\,(1-\Gamma_{@P_p})}\,P_p\right] - \left[\frac{\dot{m}}{\rho_L\,(1-\Gamma_{@pipe})}\,c_{pipe}\dot{m}^{\xi_{pipe}}\right] - \left[\frac{\dot{m}}{\rho_L\,(1-\Gamma_{@ann})}\,c_{ann}\dot{m}^{\xi_{ann}}\right]$$

$$HP_{\Delta P_b} = \left[\frac{\dot{m}}{\rho_L\,(1-\Gamma_{@P_p})}\,P_p\right] - \left[\frac{\dot{m}^{1+\xi_{pipe}}}{\rho_L\,(1-\Gamma_{@pipe})}\,c_{pipe}\right] - \left[\frac{\dot{m}^{1+\xi_{ann}}}{\rho_L\,(1-\Gamma_{@ann})}\,c_{ann}\right]$$

When calculating for maximum hydraulic horsepower at the bit, the equation is differentiated with respect to the independent variables. Then the first derivative is set to zero.

$$\frac{\partial HP_b}{\partial \dot{m}} = 0$$

$$\frac{\partial^2 HP_b}{\partial \dot{m}^2} < 0$$

$$\frac{\partial HP_b}{\partial \dot{m}} = 0 = \left[\frac{P_p}{\rho_L\,(1-\Gamma_{@P_p})}\right] - \left[\frac{(1+\xi_{pipe})\dot{m}^{\xi_{pipe}}}{\rho_L\,(1-\Gamma_{@pipe})}\,c_{pipe}\right] - \left[\frac{(1+\xi_{ann})\dot{m}^{\xi_{ann}}}{\rho_L\,(1-\Gamma_{@ann})}\,c_{ann}\right]$$

$$0 = \left[\frac{P_p}{\rho_L\,(1-\Gamma_{@P_p})}\right] - \left[\frac{(1+\xi_{pipe})}{\rho_L\,(1-\Gamma_{@pipe})}\,\Delta P_{f_{pipe}}\right] - \left[\frac{(1+\xi_{ann})}{\rho_L\,(1-\Gamma_{@ann})}\,\Delta P_{f_{ann}}\right]$$

The equation reduces to;

$$P_p = \left[\frac{(1+\xi_{pipe})}{\rho_L\,(1-\Gamma_{@pipe})}\,\Delta P_{f_{pipe}} + \frac{(1+\xi_{ann})}{\rho_L\,(1-\Gamma_{@ann})}\,\Delta P_{f_{ann}}\right]\rho_L\,(1-\Gamma_{@P_p})$$

Also, the pressure loss in the circulation system is;

$$\frac{\Delta P_f}{\Delta L} = \frac{2\,f_f \rho V^2}{D} \quad \text{----------(Eq. 4.26)}$$

Arranging this for mass rate yields;

$$\dot{m} = Q\rho = VA\rho \quad \text{(Eq. 4.27)}$$

$$V = \frac{\dot{m}}{A\rho_L(1-\Gamma)}$$

$$A = \frac{\pi}{4}D^2$$

$$\frac{\Delta P_f}{\Delta L} = \frac{32\, f_f \rho_L (1-\Gamma)\dot{m}^2}{D^5\pi^2{\rho_L}^2(1-\Gamma)^2}$$

$$\Delta P_f = \frac{32\, f_f \dot{m}^2}{D^5\pi^2\rho_L\,(1-\Gamma)}\Delta L$$

Friction factor should be determined accordingly with the flow regime. For laminar flow;

$$f_f = \frac{16}{N_{RE}}$$

For turbulent flow;

$$f_f = \frac{0.0791}{{N_{RE}}^{0.25}} \quad \text{(Eq. 4.28)}$$

Where;

$$N_{RE} = \frac{V\rho D}{\mu} = \frac{\dot{m}}{\frac{\pi}{4}D^2\rho_L\,(1-\Gamma)} \times \frac{\rho_L\,(1-\Gamma)D}{\mu}$$

$$N_{REM} = \frac{4\dot{m}}{\pi D\mu_e} \quad \text{(Eq. 4.29)}$$

As the mass rate is a function of flow rate;

$$\Delta P_f\big|_{\Gamma} = c\,\dot{m}^{\xi}$$

$$\left.\frac{\Delta P_{f_1}}{\Delta P_{f_2}}\right|_{\Gamma} = \left[\frac{\dot{m}_1}{\dot{m}_2}\right]^{\xi}$$

$$\ln\frac{\Delta P_{f_1}}{\Delta P_{f_2}} = \xi \ln\frac{\dot{m}_1}{\dot{m}_2}$$

$$\xi = \frac{\ln\frac{\Delta P_{f_1}}{\Delta P_{f_2}}}{\ln\frac{\dot{m}_1}{\dot{m}_2}}$$

$$c = \frac{\Delta P_{f_1}}{\dot{m}_1{}^{\xi}}$$

$$for\ \xi_p \rightarrow use\ \Gamma_{pipe}$$

$$for\ \xi_a \rightarrow use\ \Gamma_{annnulus}$$

4.3. COMPUTER WORK

In this study, the mathematical model was constructed using the mass flow rate of the foams. A computer program was developed based on this mathematical model using the programming language "C".

This programming language was selected mainly because it is the most common programming language and also because it is user friendly. The program is easier to develop because it can be developed in modules and this enables it to be much simpler to follow. Another major advantage to the program is that it does not require too much memory from the computer and it can work in any computer system.

4.3.1 Assumptions

The assumptions that were used when developing this model were:

- The wellbore geometry is uniform and constant.
- The drillstring geometry is uniform and constant.
- The wellbore is vertical.
- The temperature increase in the system is linear.
- The formation fluid influx is negligible.
- The rheology of foam may be characterized using Power-law model.
- Maximum cleaning of the wellbore will be achieved by providing the maximum horsepower to the bit.
- A tri-cone bit with 3 nozzles is used for the drilling operation.
- Pressure drops at the surface system are negligible.

4.3.2 Input

When the computer program is run, it first asks for the data it requires from the user in order to perform the calculations. **Table 4** shows the type and the units of data input required from the user.

Table 4 Input Data for the Program

Data Type	Unit
Inner Pipe Diameter	Inch
Outer Pipe Diameter	Inch
Hole Diameter	Inch
Hole Depth	Feet
Temperature Gradient	^{o}F / 100 feet
Formation Pressure	Psi
Maximum Inlet Pressure	Psi

4.3.3 Output

The program generates the output data shown in **Table 5**.

Table 5 Output Data for the Program

Data Type	Unit
Bottomhole Pressure	Psi
Bottomhole Temperature	^{o}F
Static Backpressure	Psi
Bit Pressure Loss	Psi
Frictional Pressure Loss Inside String	Psi
Frictional Pressure Loss Inside Annulus	Psi
Bottomhole Foam Velocity	feet/sec
Bottomhole Foam Quality	%
Optimum Gas Flow Rate	Scfm
Optimum Liquid Flow Rate	Gpm
Optimum Nozzle Size	32^{nd} s of inch

4.3.4 Methodology

- The input values that are entered in conventional field units are simultaneously converted to values with units that will be used in the mathematical formulations through the program.
- Beginning with a nozzle size of 8/32 inch the minimum and the maximum mass rate capacities are defined for the annulus considering water as the liquid phase and air as the gaseous phase.
- The dynamic backpressure at the depth of interest is calculated. This value in turn is used for the calculation of the hydrostatic pressure.
- The annular foam quality is calculated using the hydrostatic pressure and the liquid density considering the gas density is negligible.
- In a separate subroutine bottom hole temperature, average pressure and the annular foam quality are calculated. The total flow rates, the gas rates, the foam velocity and shear rates are also determined in this section.
- The shear rate values and the qualities are sent to another subroutine where the viscosity value is calculated using equations based on the empirical values of the studies by Okpobiri and Ikoku[11].
- The friction factor is calculated using the Reynolds number which in turn is used for the pressure drop in the annulus.
- The bit pressure drop is calculated in a separate subroutine based on the nozzle area, the foam velocity, the mass rate of the liquid phase and the mass rate of the gaseous phase.
- Pressure drop in the pipes are calculated based on the Reynolds number, the friction factor and the pipe dimensions.
- The results are printed on the screen.
- The nozzle size is increased by 2/32 inch and the procedure is repeated up to a nozzle size of 32/32 inch.

CHAPTER 5

RESULTS AND DISCUSSIONS

For illustrative purposes, the program was run for different input values and the results were compared. The first section shows the comparison of the results from the model to the previous models. The following four sections are sensitivity analysis of the results for different hole sizes, pressure gradients, temperature gradients and nozzle sizes. The selected hole sizes were 8 ½" and 12 ¼" respectively. The pressure gradients were 0.15 psi/ft and 0.125 psi/ft for stimulating the underbalanced conditions, these values are actual field values from the Moomba field[30], Australia. Temperature gradients were 1.5 ^{o}F/100ft and 3.0 ^{o}F/100ft, and the nozzle sizes were $^{10}/_{32}$", $^{14}/_{32}$" and $^{18}/_{32}$". The change of pressure and temperature values with depth is shown in **Figure 7**. The comparisons were based on pipe ID and OD of 3.76" and 4.5" respectively, for the second, third and fourth parts $^{14}/_{32}$" nozzle size was used as a reference point. The fifth section accounts for the nozzle size change and sixth section present the other results generated by the program.

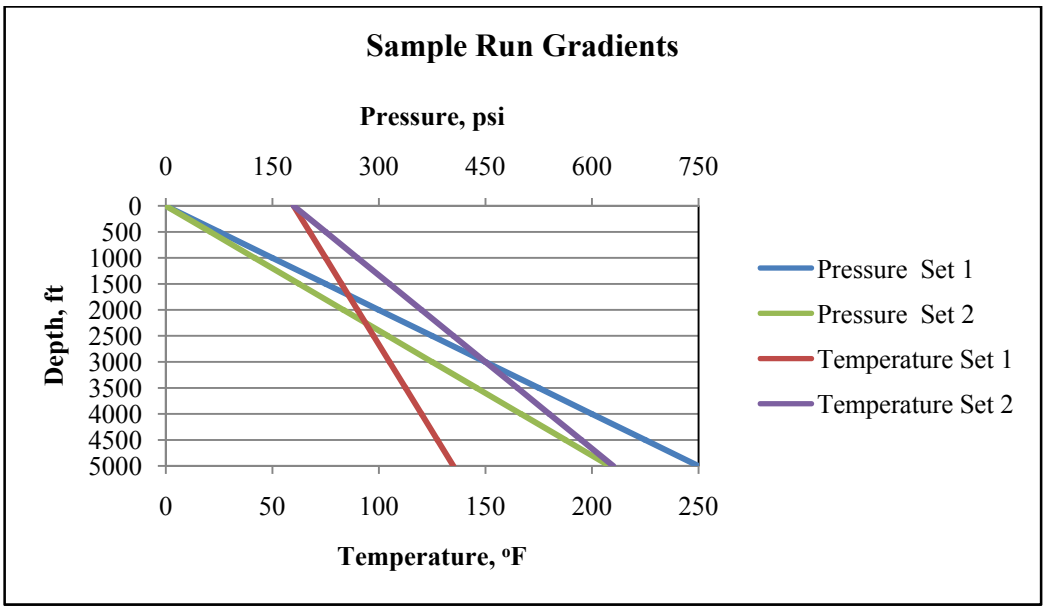

Figure 7 Pressure and Temperature Gradients for the Sample Runs

5.1. COMPARISON WITH OTHER MODELS

One of the most recognized and widely used work in the literature for foam is the model by Okpobiri and Ikoku[11]. The proposed model was also run using their set of data and the results were compared. The model of Krug and Mitchell[31] was also used in the comparison.

Plots of the liquid flow rate versus depth (**Figure 8**) and the gas flow rate versus depth (**Figure 9**) are shown below. The proposed model stays inside the area between the two models for the liquid flow rate and it also is overlying the two models for most part in the gas flow rate.

The variation may be occurring as a result of one important difference between the models, Okpobiri and Ikoku[11] assumes that the pressure losses resulting from friction and change in elevation negligible. However; proposed model has taken this loss into account.

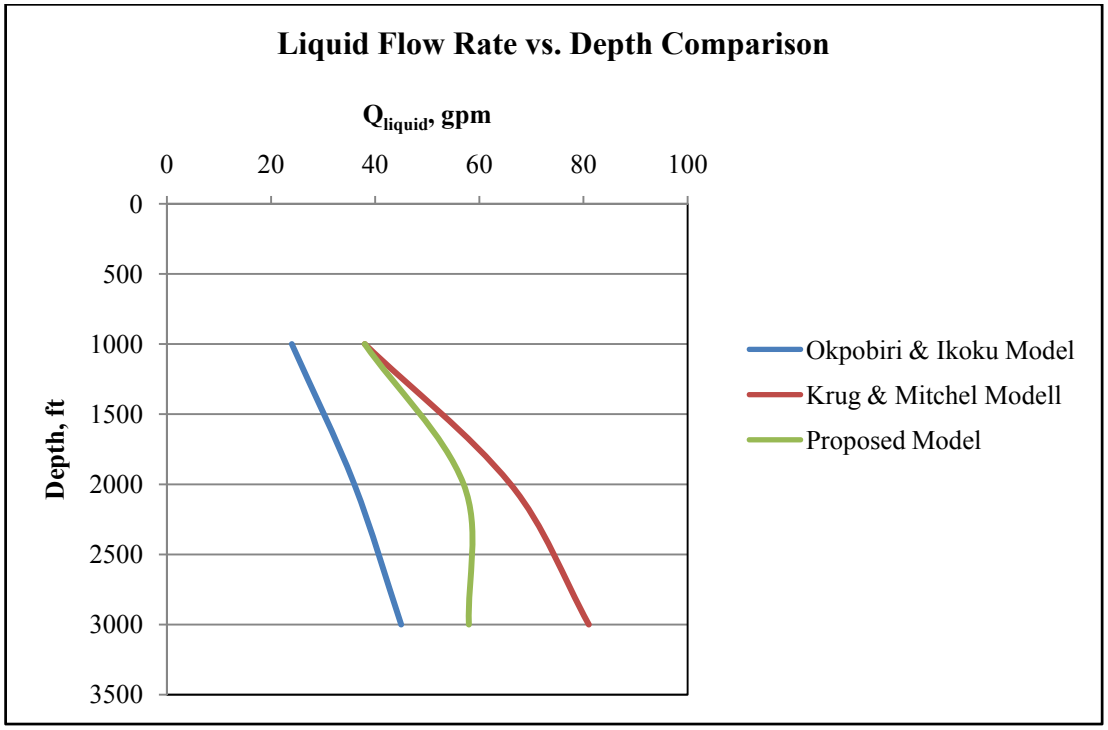

Figure 8 Comparison of Liquid Flow Rate vs. Depth Between the Models

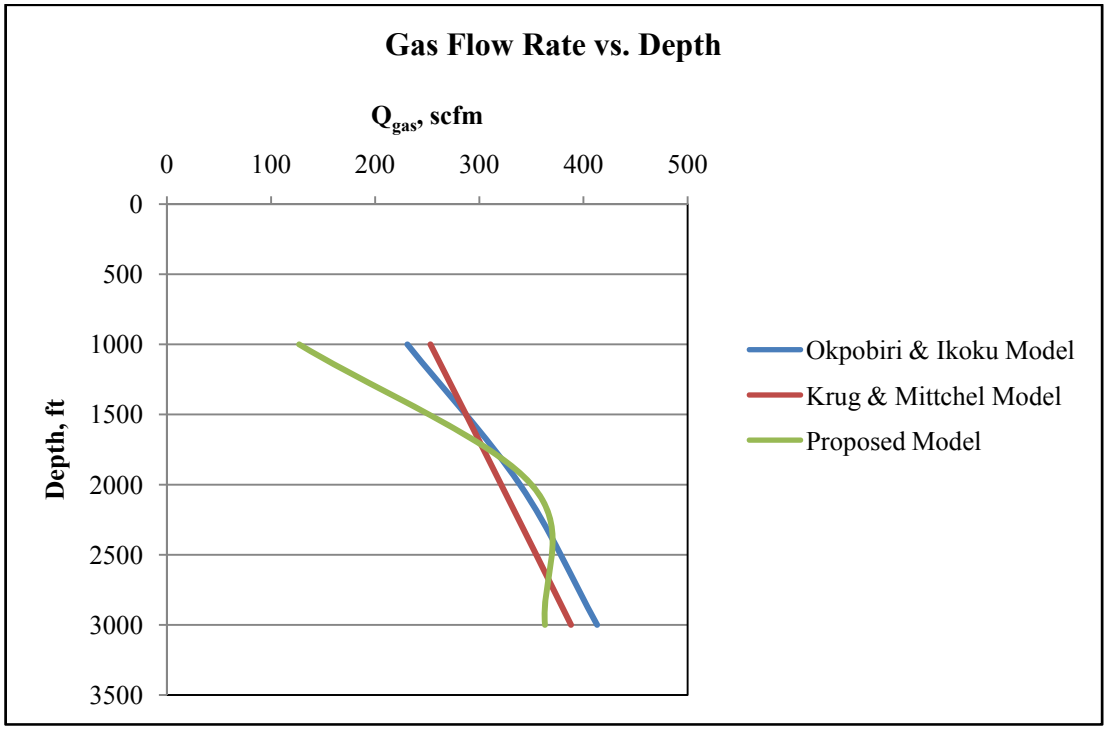

Figure 9 Comparison of Gas Flow Rate vs. Depth Between the Models

5.2. EFFECTS OF CHANGE IN HOLE SIZE

Figures 10 to 17 show the graphs for the output values of the model for 8 ½" and 12 ¼" hole sizes versus depth with 0.15 psi/ft pressure gradient, 1.5 ^{o}F/100ft temperature gradient and $^{14}/_{32}$" nozzle size. The considered data sets are shown in **Tables 6** and **7**.

Table 6 Depth Related Input for Hole Size Sensitivity Runs

Depth	**P Inlet**	**P Formation**	**Temp.**
(feet)	**(psi)**	**(psi)**	**(^{o}F)**
500,00	52,50	75,00	67,50
1000,00	105,00	150,00	75,00
1500,00	157,50	225,00	82,50
2000,00	210,00	300,00	90,00
2500,00	262,50	375,00	97,50
3000,00	315,00	450,00	105,00
3500,00	367,50	525,00	112,50
4000,00	420,00	600,00	120,00
4500,00	472,50	675,00	127,50
5000,00	525,00	750,00	135,00

Table 7 Other Input for Hole Size Sensitivity Runs

	RUN1	**RUN2**
PIPE ID (in)	3,76	3,76
PIPE OD (in)	4,50	4,50
HOLE D (in)	8,50	12,25
NOZZLE (in/32)	14,00	14,00
P Grad (psi/ft)	0,15	0,15
T Grad (F/100ft)	1,50	1,50

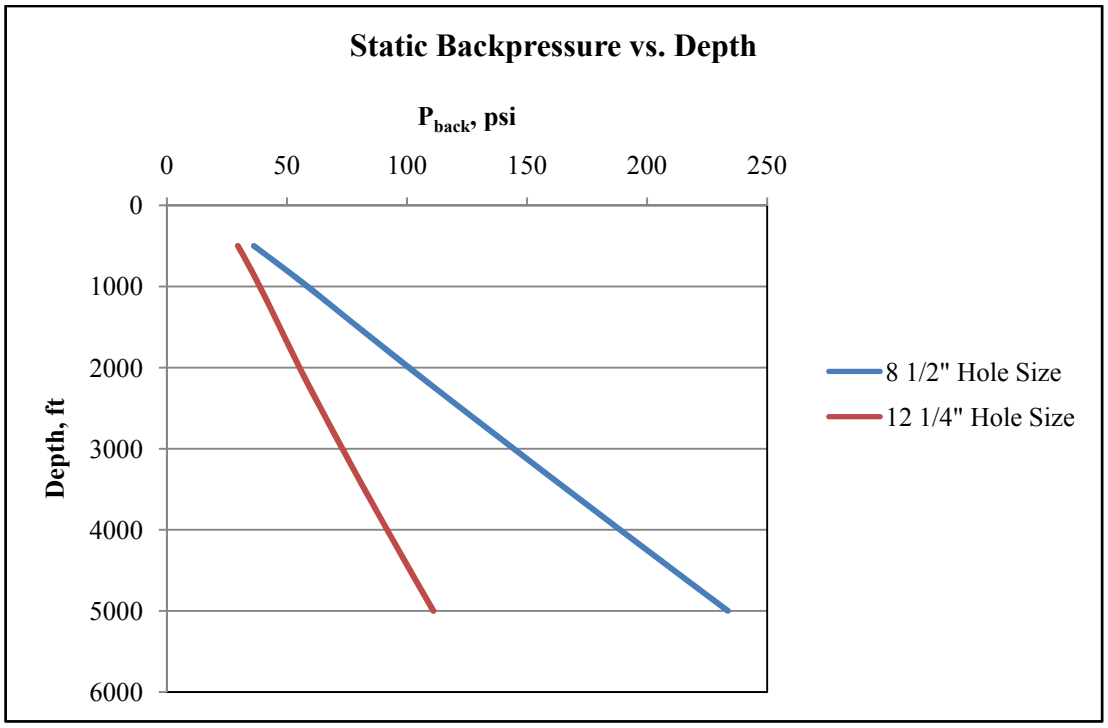

Figure 10 Change of Static Backpressure with Depth and Hole Size

The static backpressure trend for the 8 ½" hole size is higher compared to the trend for the 12 ¼" hole size (**Figure 10**). The backpressure was expected to increase with decreasing hole size, which is similar to the behavior of backpressure seen in the paraffinic petroleum flow lines with reduced diameter during cold days. The proposed model was successful in defining this relation.

The larger hole size yields more pressure loss at the bit (**Figure 11**). The pressure drop at the bit depends on the flow rate. Changing the hole diameter also means changing the flow rates and thus the pressure loss at the bit changes.

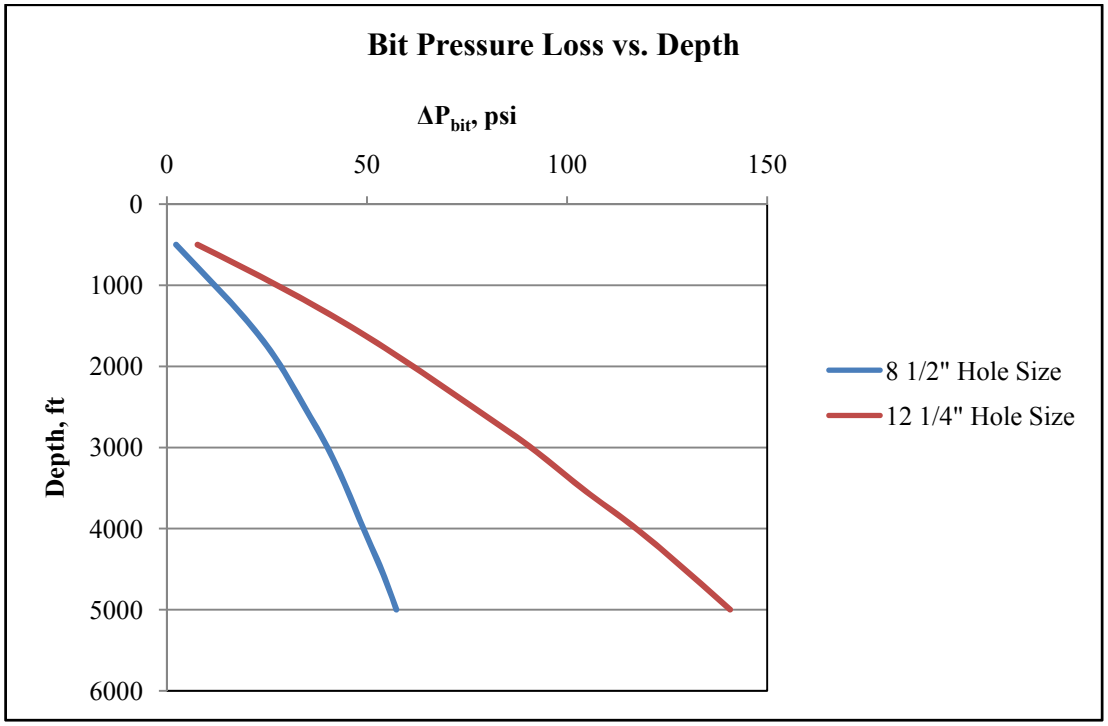

Figure 11 Change of Bit Pressure Loss with Depth and Hole Size

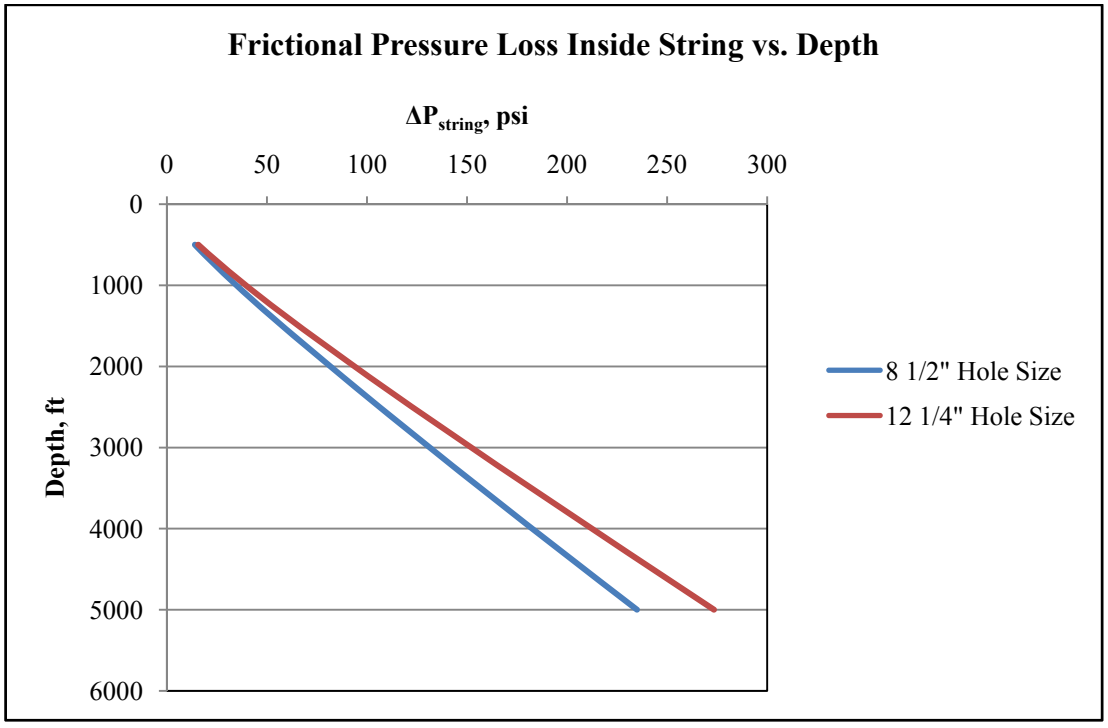

Figure 12 Change of Frictional Pressure Loss Inside String with Depth and Hole Size

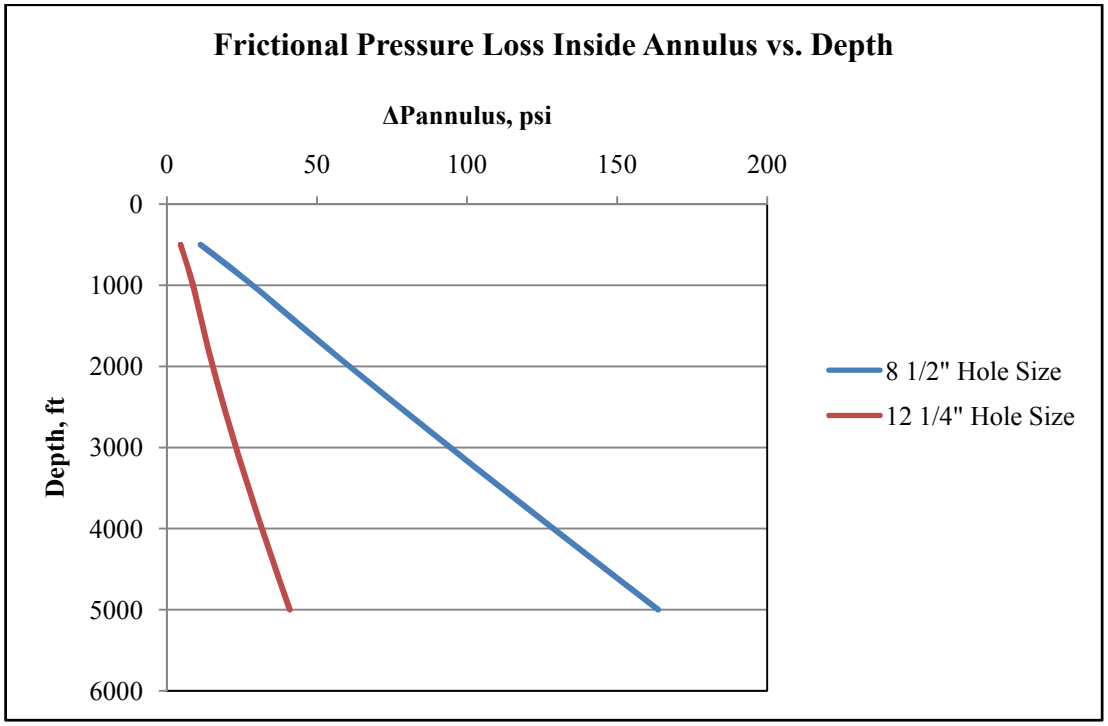

Figure 13 Change of Frictional Pressure Loss Inside Annulus with Depth and Hole Size

Figures 12 and 13 show the change in the frictional pressure loss inside the string and inside the annulus by changing the hole size. The pressure loss in the string is higher for the larger hole. This change is because of the increase in the foam density as a result of change in the foam quality. The pressure loss inside the annulus on the other hand decreases with increasing hole size as it is inversely proportional to the flow area.

The foam velocity and the foam quality both decrease with the increasing hole size (**Figures 14 and 15**) as expected. Also, in order to deliver the maximum horsepower to the bit, the optimum flow rate for liquid (**Figure 16**) and the optimum flow rate for gas (**Figure 17**) increases as the volume also increases. However, one must keep in mind that the comparison is for $^{14}/_{32}$" nozzle size and the hole sizes, not the hydraulics in this case, and the model is successful in defining the change in the output as a result of the change in the hole size.

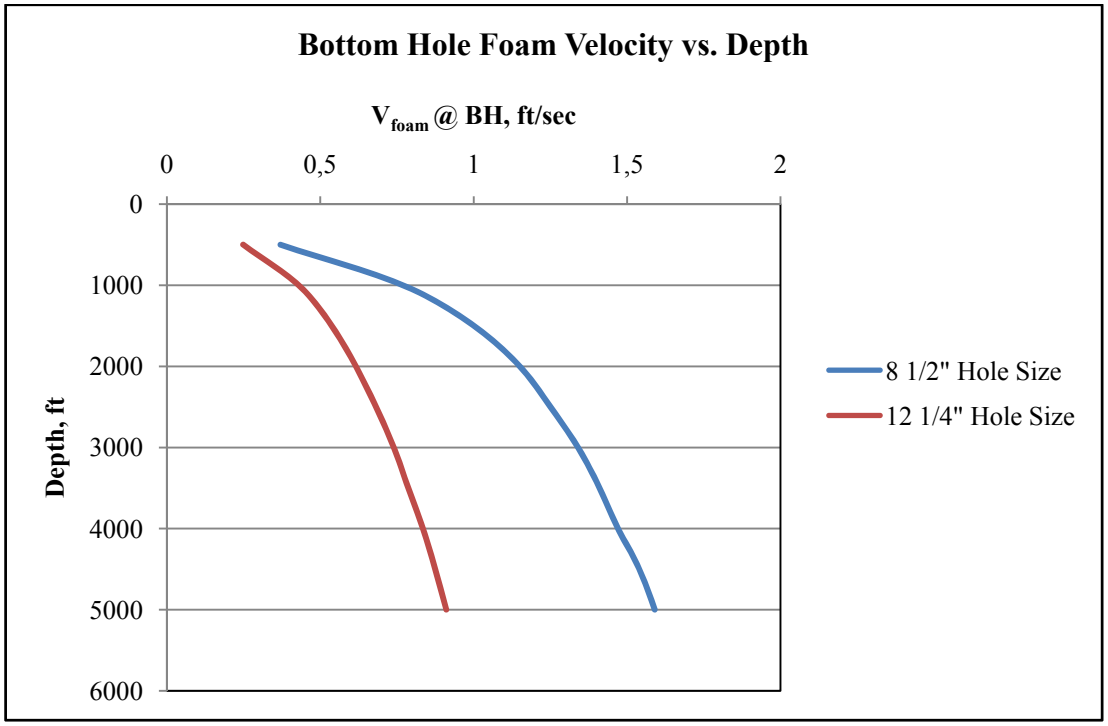

Figure 14 Change of Bottom Hole Foam Velocity with Depth and Hole Size

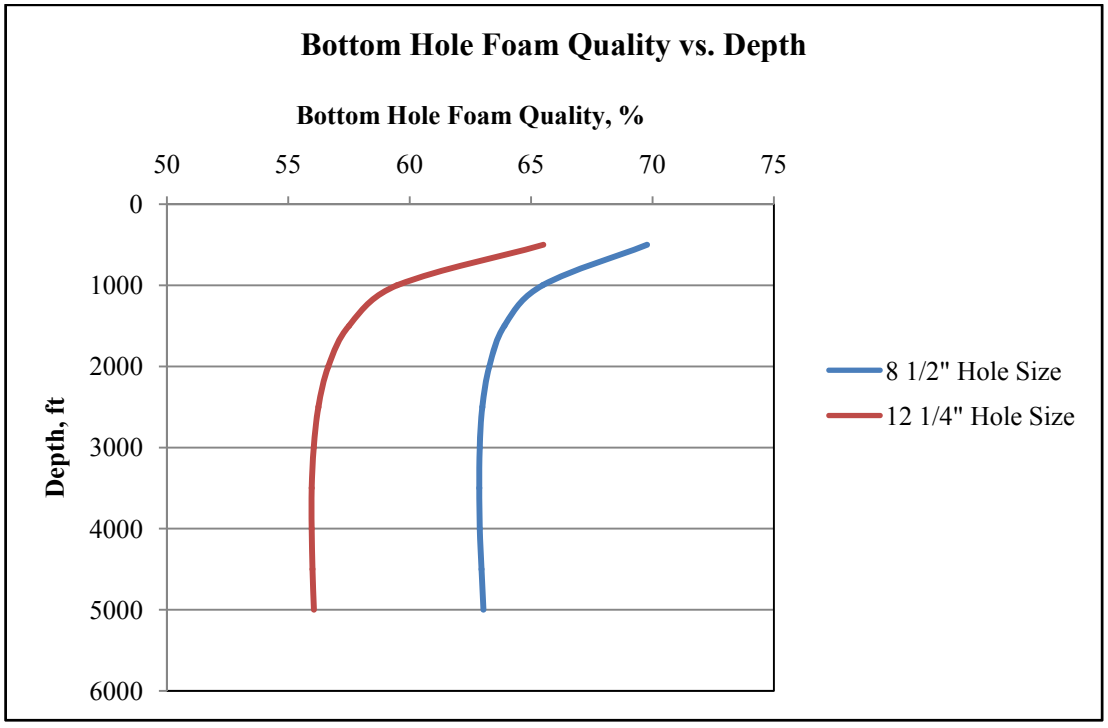

Figure 15 Change of Bottom Hole Foam Quality with Depth and Hole Size

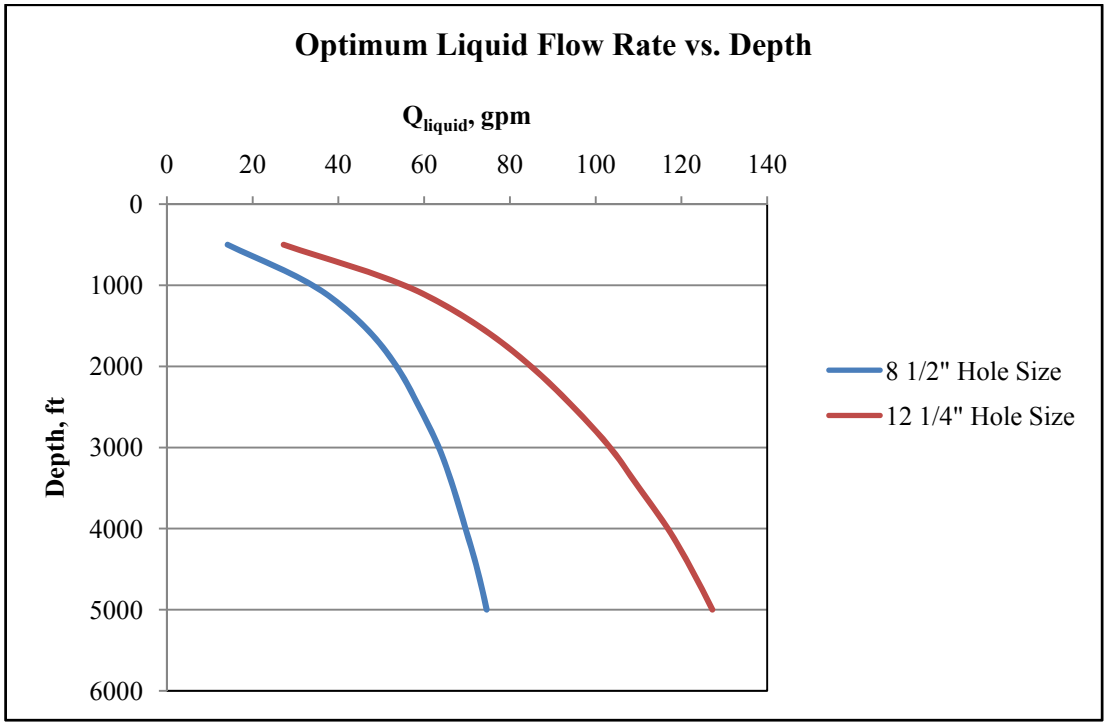

Figure 16 Change of Optimum Liquid Flow Rate with Depth and Hole Size

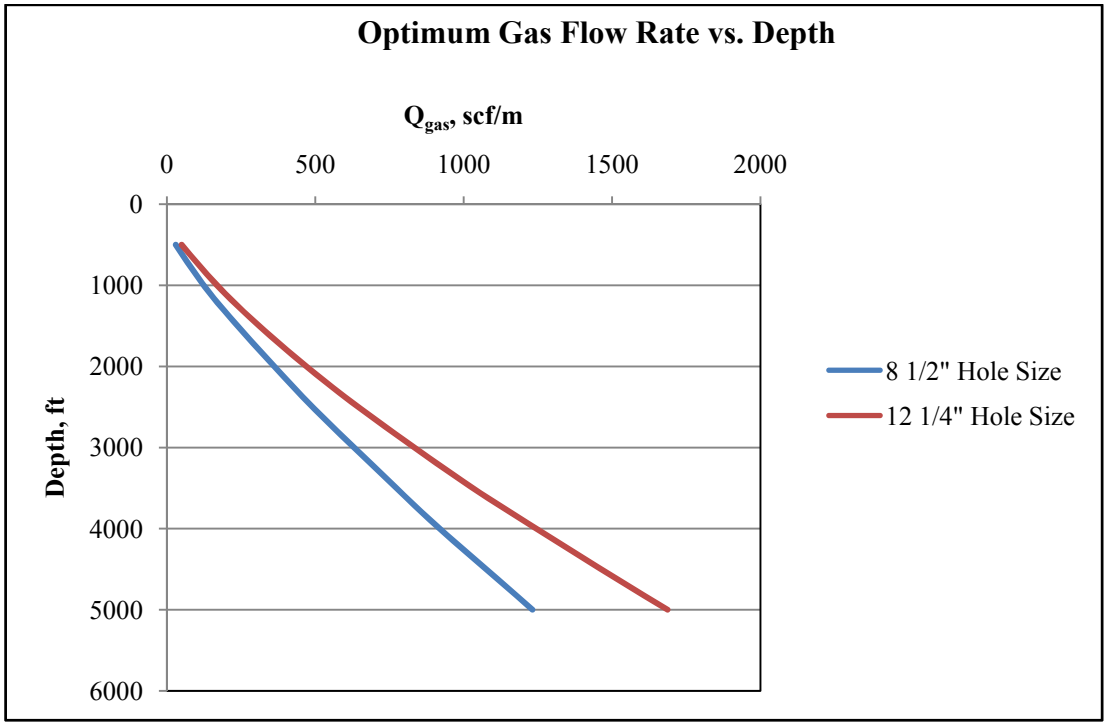

Figure 17 Change of Optimum Gas Flow Rate with Depth and Hole Size

5.3. EFFECTS OF CHANGE IN PRESSURE GRADIENT

Figures 18 to 25 show the graphs for the output values of the model for 0.15 psi/ft and 0.125 psi/ft pressure gradients versus depth with the 8 ½" hole size, 1.5 ^{o}F/100ft temperature gradient and $^{14}/_{32}$" nozzle size. Data sets used for this analysis are shown in **Tables 8** and **9**.

Table 8 Depth Related Input for Pressure Gradient Sensitivity Runs

Depth (feet)	P Inlet (psi) RUN1	P Formation (psi) RUN1	P Inlet (psi) RUN2	P Formation (psi) RUN2	Temp. (^{o}F)
500,00	52,50	75,00	43,75	62,50	67,50
1000,00	105,00	150,00	87,50	125,00	75,00
1500,00	157,50	225,00	131,25	187,50	82,50
2000,00	210,00	300,00	175,00	250,00	90,00
2500,00	262,50	375,00	218,75	312,50	97,50
3000,00	315,00	450,00	262,50	375,00	105,00
3500,00	367,50	525,00	306,25	437,50	112,50
4000,00	420,00	600,00	350,00	500,00	120,00
4500,00	472,50	675,00	393,75	562,50	127,50
5000,00	525,00	750,00	437,50	625,00	135,00

Table 9 Other Input for Pressure Gradient Sensitivity Runs

	VALUE
PIPE ID (in)	3,76
PIPE OD (in)	4,50
HOLE D (in)	8,50
NOZZLE (in/32)	14,00

Figures 18 to 21 depict the changes in the pressure losses in the system. The static backpressure and pressure losses inside the annulus are not changing significantly as a result of a change in the pressure gradient mainly because the hole size is constant and also because the inlet pressures are assumed same for both pressure gradients.

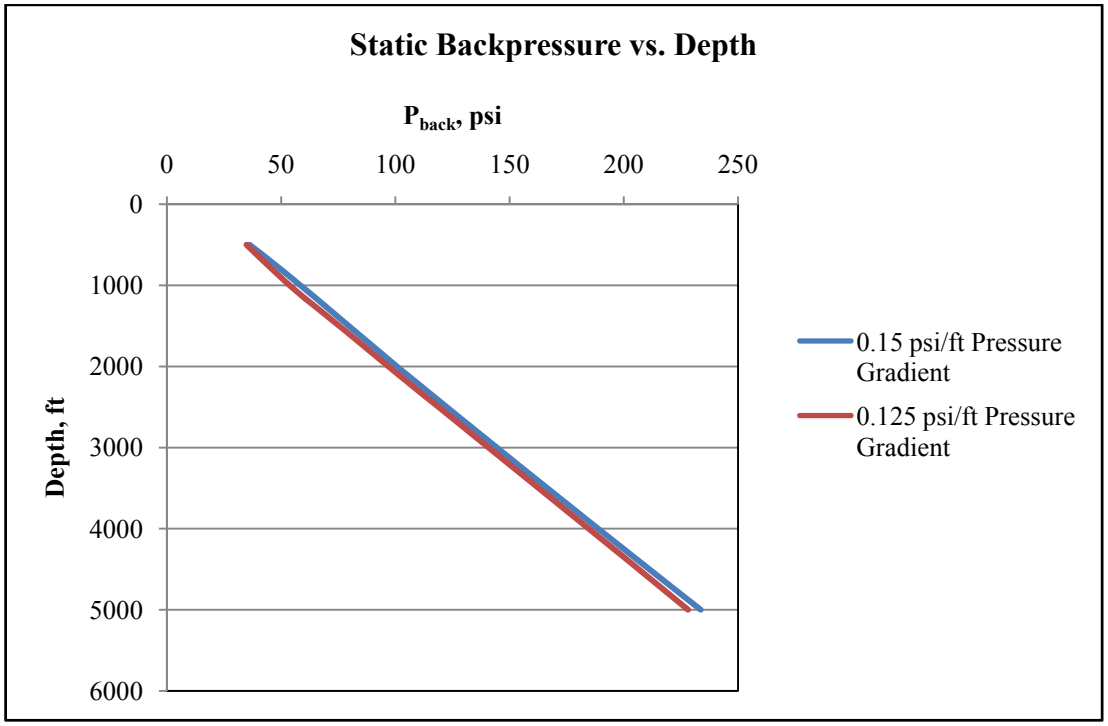

Figure 18 Change of Static Backpressure with Depth and Pressure Gradient

The bit pressure loss decreases significantly, mostly because of the decrease in the velocity, and thus the flow rate. The decrease of the pressure loss inside the string can be explained similarly.

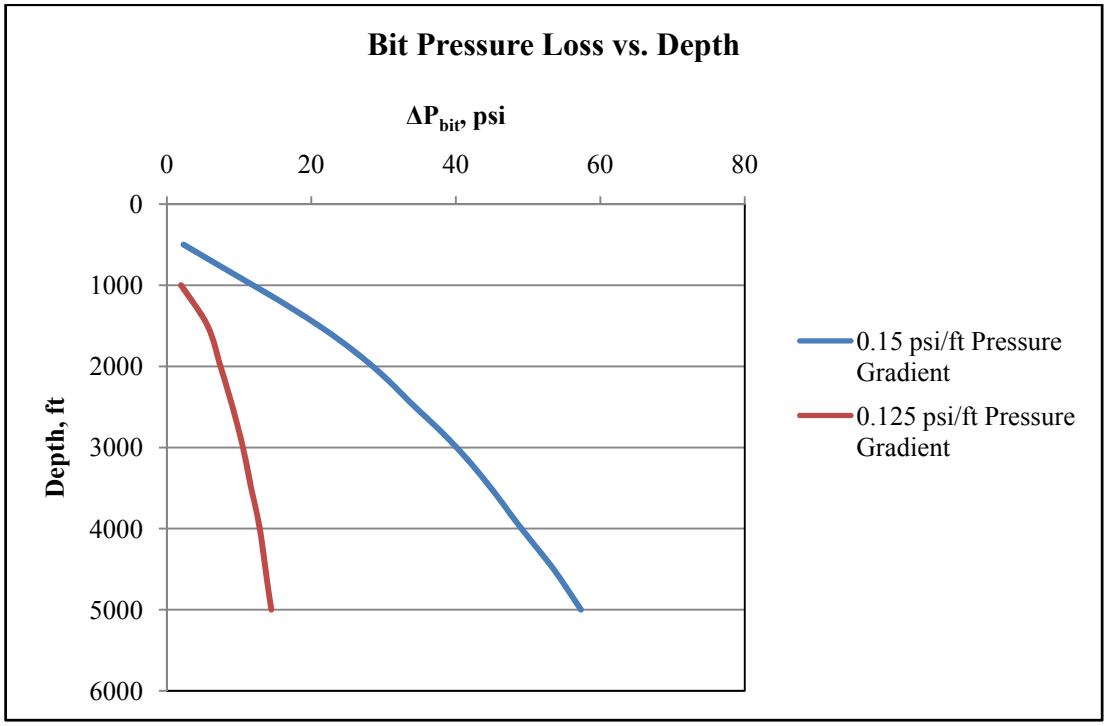

Figure 19 Change of Bit Pressure Loss with Depth and Formation Pressure Gradient

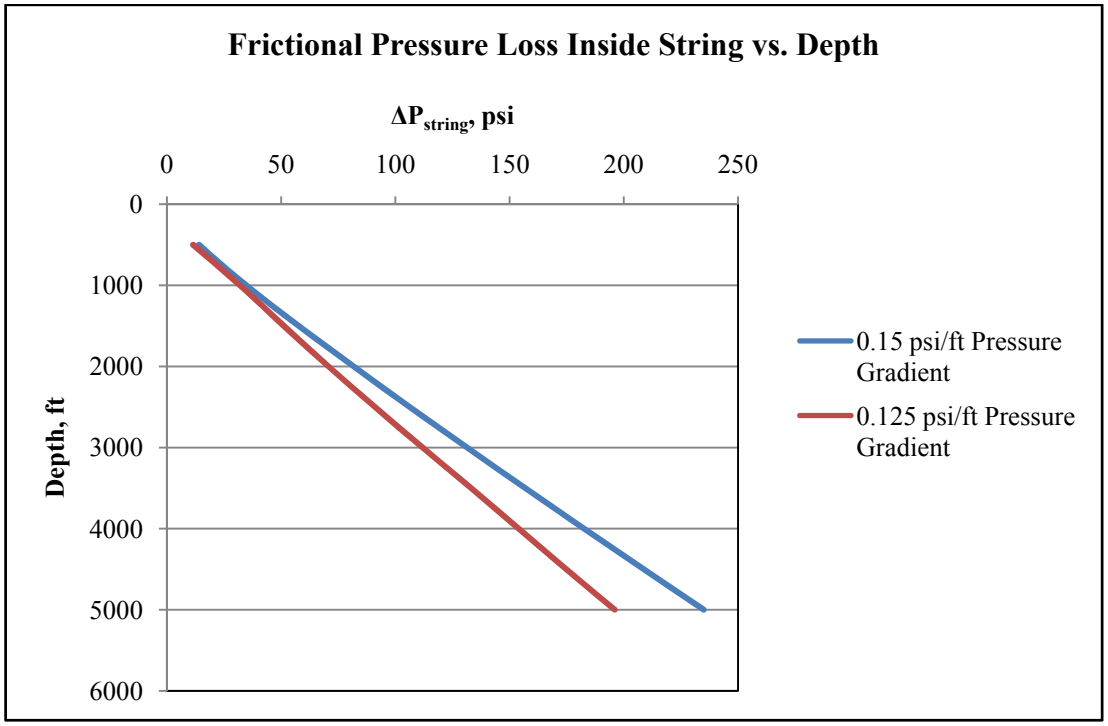

Figure 20 Change of Frictional Pressure Loss Inside String with Depth and Formation Pressure Gradient

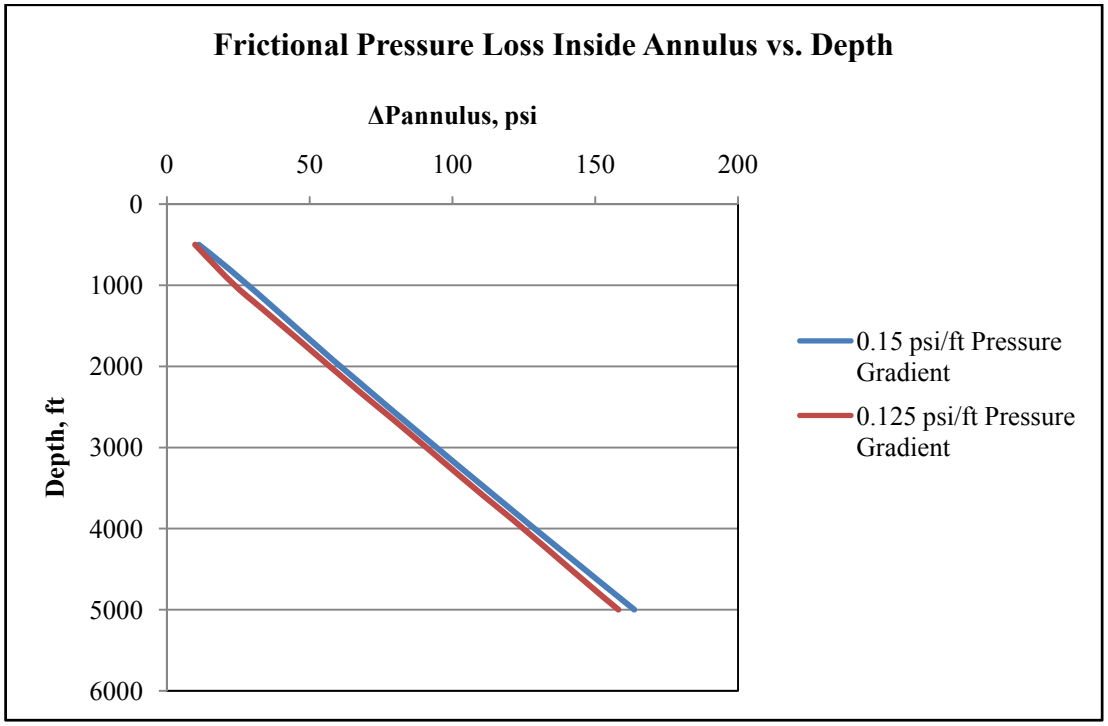

Figure 21 Change of Frictional Pressure Loss Inside Annulus with Depth and Formation Pressure Gradient

The bottom hole foam velocity increases with the increasing pressure gradient (**Figure 22**). The foam velocity depends on the mass rate, thus the change can easily be explained by the increase in the optimum liquid flow rate (**Figure 24**) and the increase in the optimum gas flow rate (**Figure 25**) with increasing pressure requirement and the $^{14}/_{32}$" nozzle size.

There is an increase in the foam quality (**Figure 23**) for lower pressure gradients. Overall, the model was also successful in defining the change in the output as a result of the change in the pressure gradient.

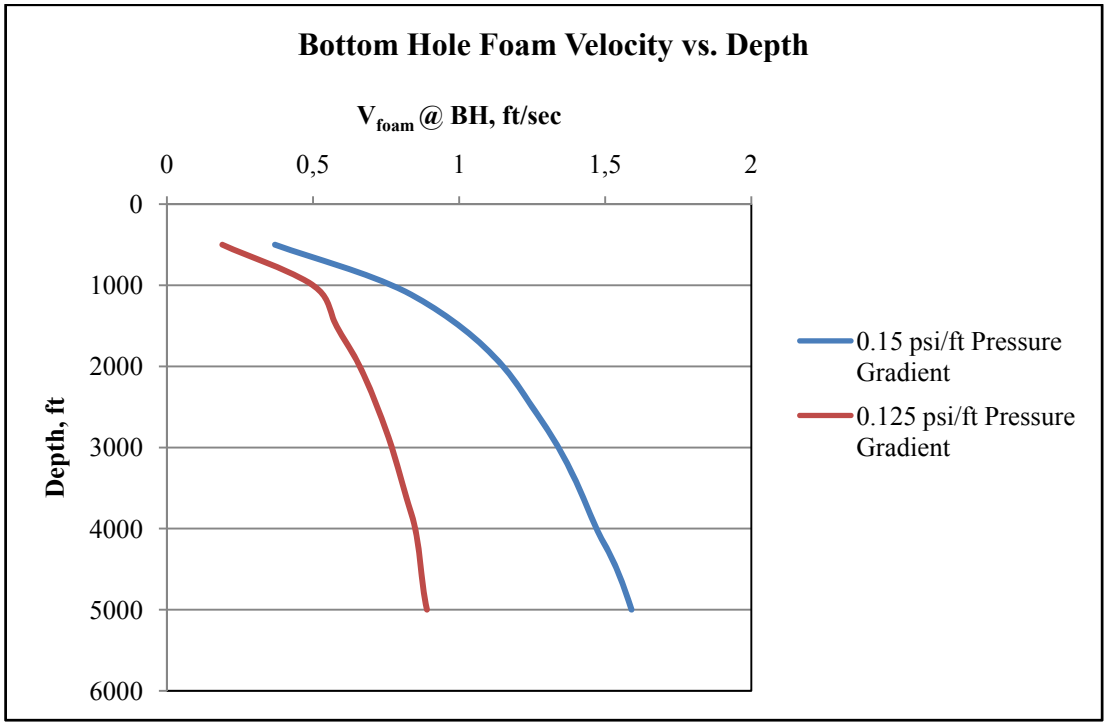

Figure 22 Change of Bottom Hole Foam Velocity with Depth and Formation Pressure Gradient

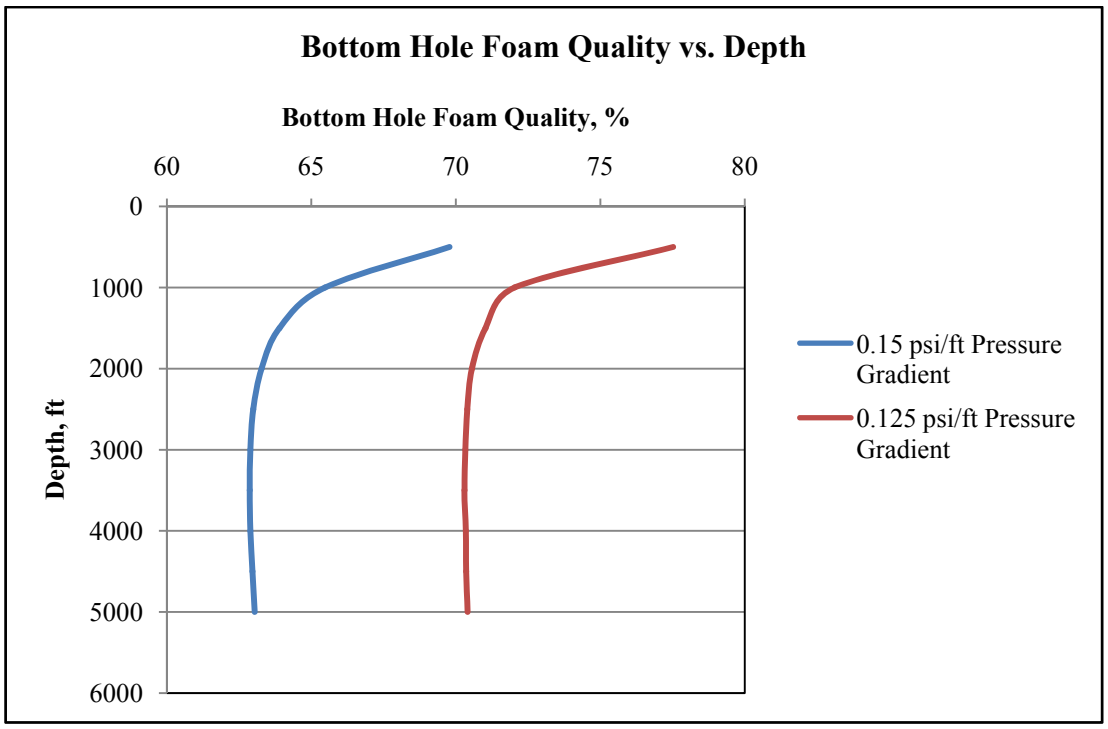

Figure 23 Change of Bottom Hole Foam Quality with Depth and Formation Pressure Gradient

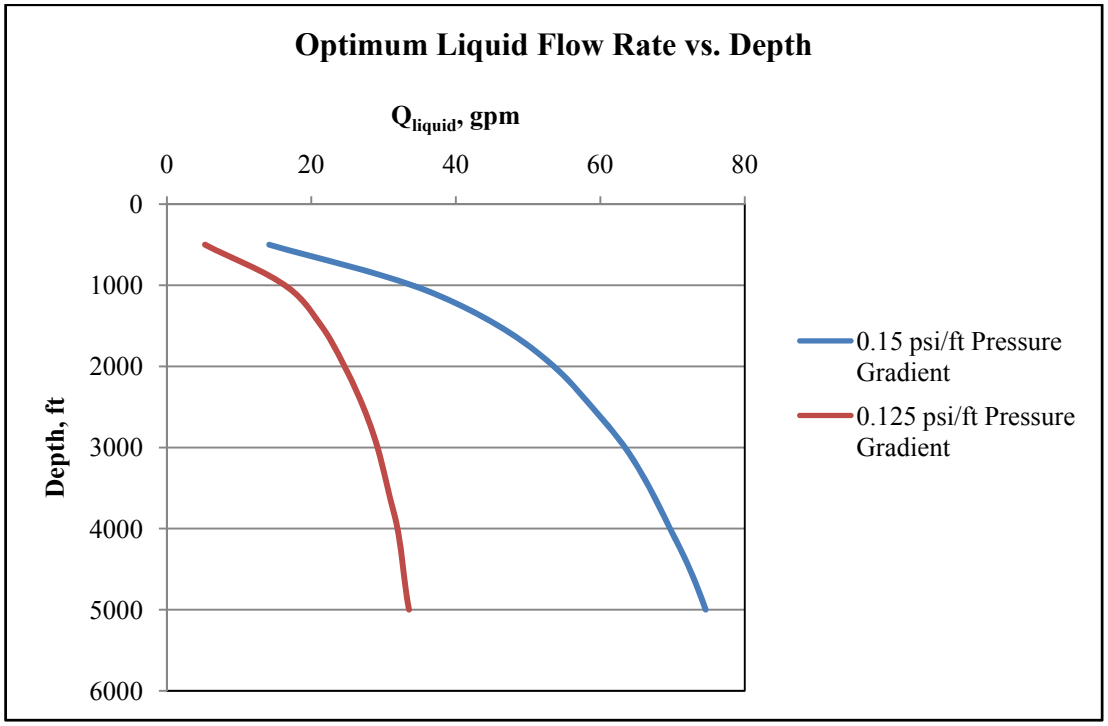

Figure 24 Change of Optimum Liquid Flow Rate with Depth and Formation Pressure Gradient

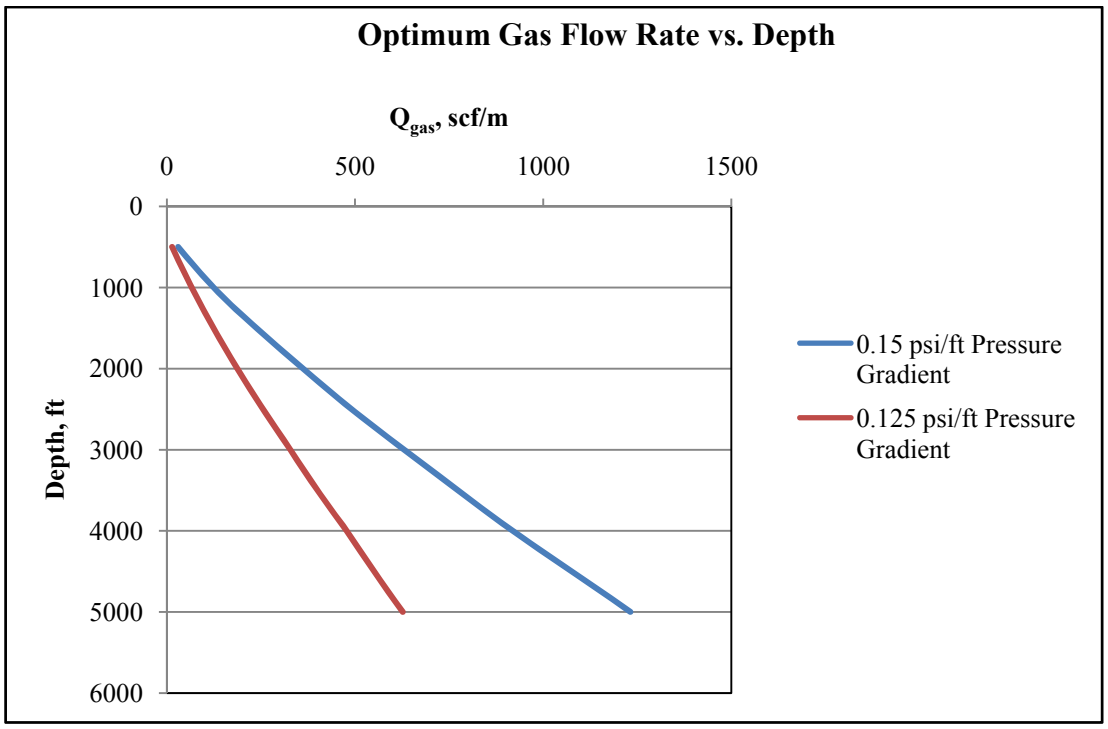

Figure 25 Change of Optimum Gas Flow Rate with Depth and Formation Pressure Gradient

5.4. EFFECTS OF CHANGE IN TEMPERATURE GRADIENT

Figures 26 to 33 show the graphs for the output values of the model for 1.5 ^{o}F/100ft and 3.0 ^{o}F/100ft temperature gradients versus depth with the 8 ½" hole size, 0.15 psi/ft pressure gradient and $^{14}/_{32}$" nozzle size. Data sets used for this analysis are shown in **Tables 10** and **11**.

Table 10 Depth Related Input for Temperature Gradient Sensitivity Runs

Depth (feet)	**P Inlet (psi)**	**P Formation (psi)**	**Temp. (^{o}F) RUN1**	**Temp. (^{o}F) RUN2**
500,00	52,50	75,00	67,50	75,00
1000,00	105,00	150,00	75,00	90,00
1500,00	157,50	225,00	82,50	105,00
2000,00	210,00	300,00	90,00	120,00
2500,00	262,50	375,00	97,50	135,00
3000,00	315,00	450,00	105,00	150,00
3500,00	367,50	525,00	112,50	165,00
4000,00	420,00	600,00	120,00	180,00
4500,00	472,50	675,00	127,50	195,00
5000,00	525,00	750,00	135,00	210,00

Table 11 Other Input for Temperature Gradient Sensitivity Runs

	VALUE
PIPE ID (in)	3,76
PIPE OD (in)	4,50
HOLE D (in)	8,50
NOZZLE (in/32)	14,00

Figures 26 to 29 show the changes in the pressure losses in the system. The pressure losses are not changing significantly as a result of a change in the temperature gradient mainly because the hole size is constant and also because the inlet pressures are assumed same for both temperature gradients.

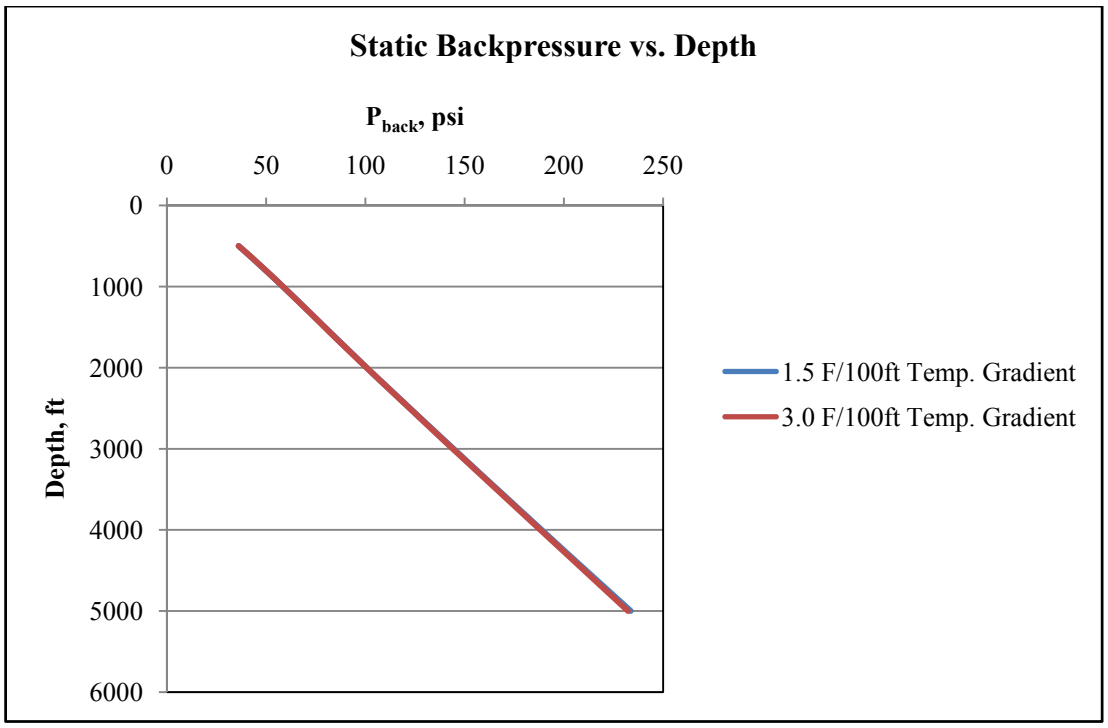

Figure 26 Change of Static Backpressure with Depth and Temperature Gradient

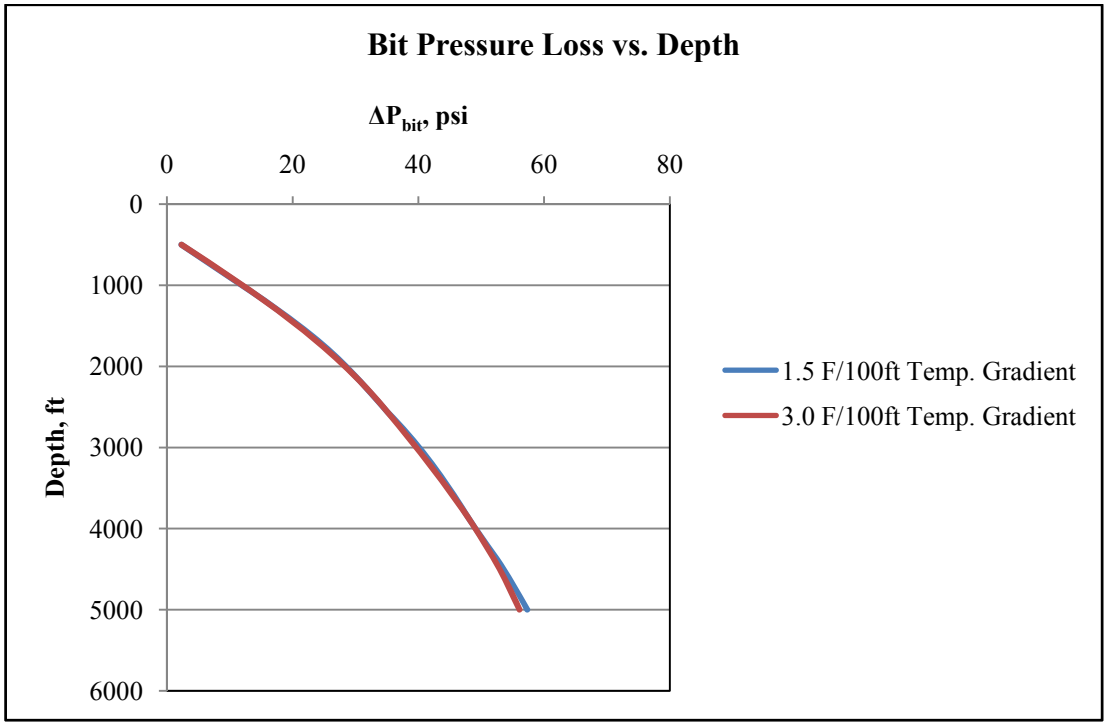

Figure 27 Change of Bit Pressure Loss with Depth and Temperature Gradient

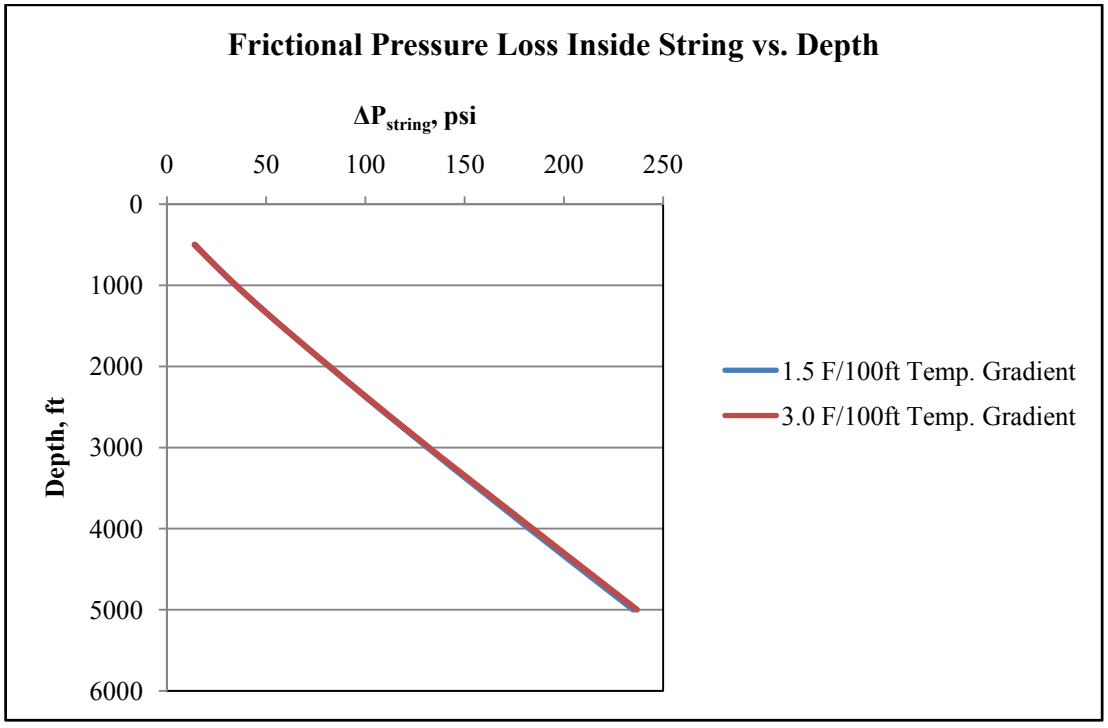

Figure 28 Change of Frictional Pressure Loss Inside String with Depth and Temperature Gradient

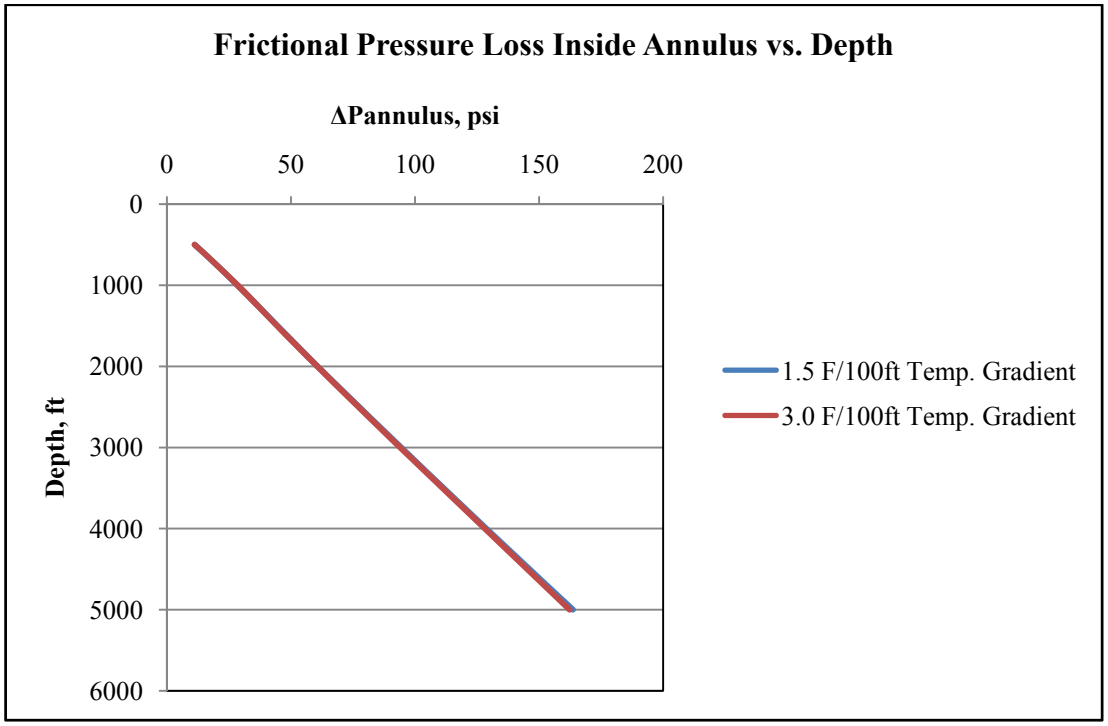

Figure 29 Change of Frictional Pressure Loss Inside Annulus with Depth and Temperature Gradient

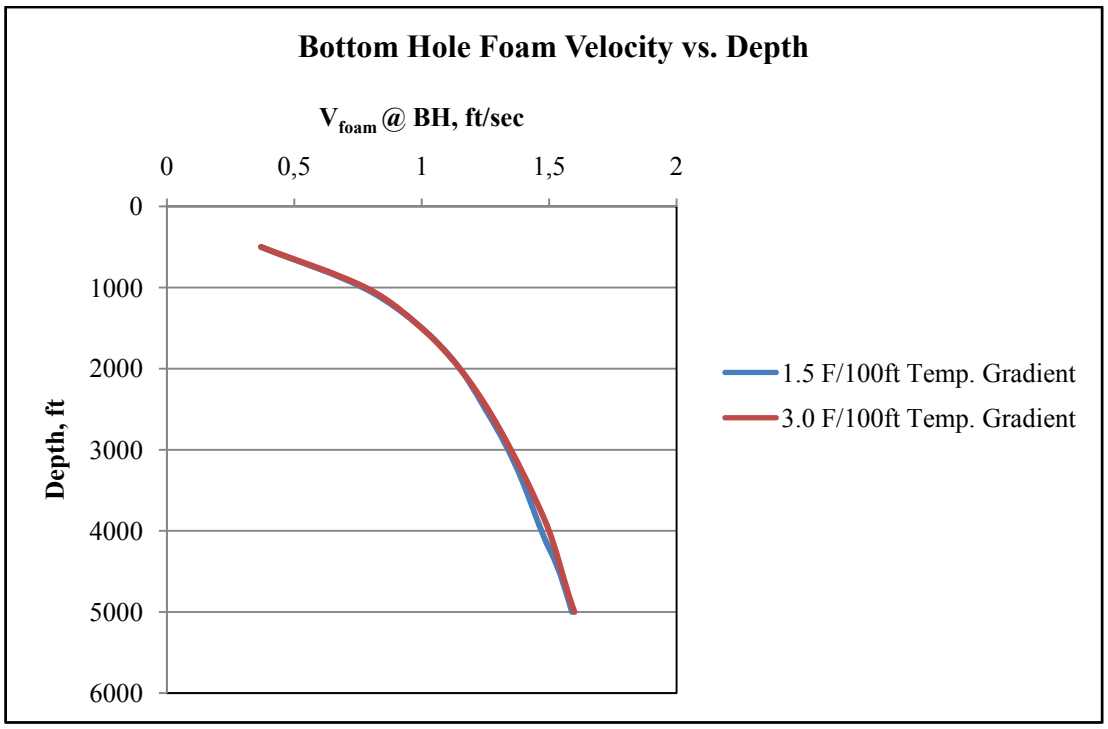

Figure 30 Change of Bottom Hole Foam Velocity with Depth and Temperature Gradient

The change in the velocity of the foam is also not significant for this case (**Figure 30**). The bottom hole foam quality on the other hand, is obviously affected by the change in the temperature gradient (**Figure 31**). This is not as a result of the change in the optimum liquid flow rates (**Figure 32**) but as a result of the change in the optimum gas flow rates (**Figure 33**) and thermal effects on gas volume. Even though there is not a significant influence of the temperature gradient in the model, temperature is one of the many factors that add up to the general result. The model is able to identify a relation and add this into the general solution.

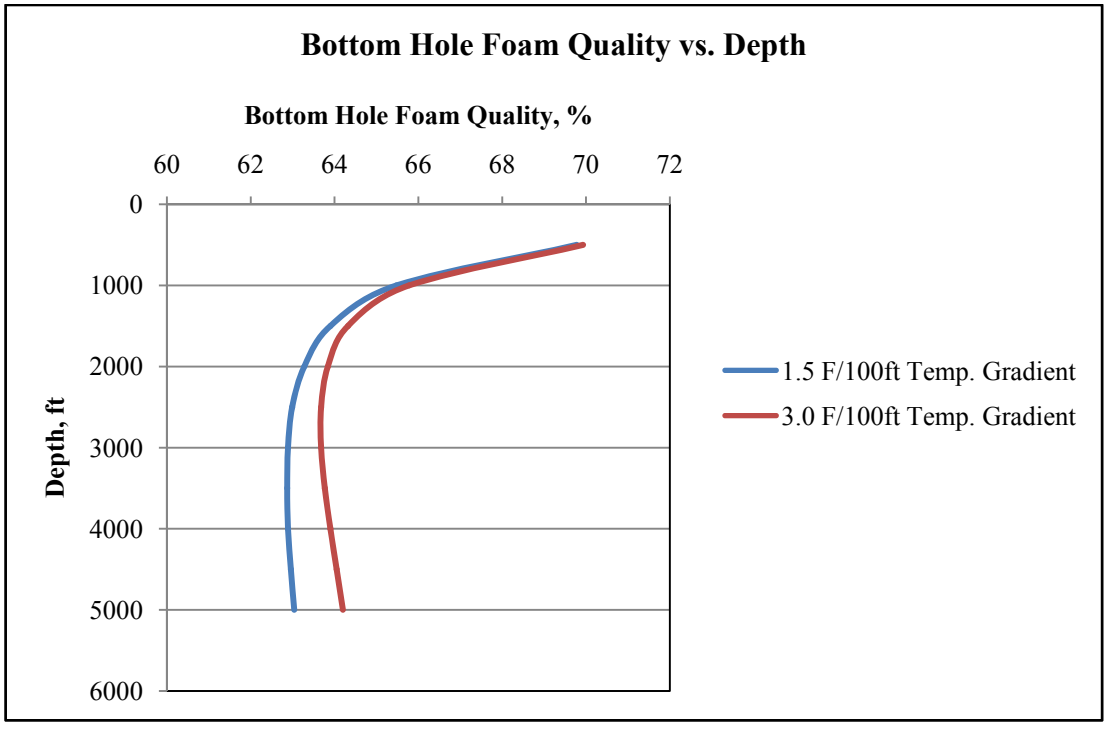

Figure 31 Change of Bottom Hole Foam Quality with Depth and Temperature Gradient

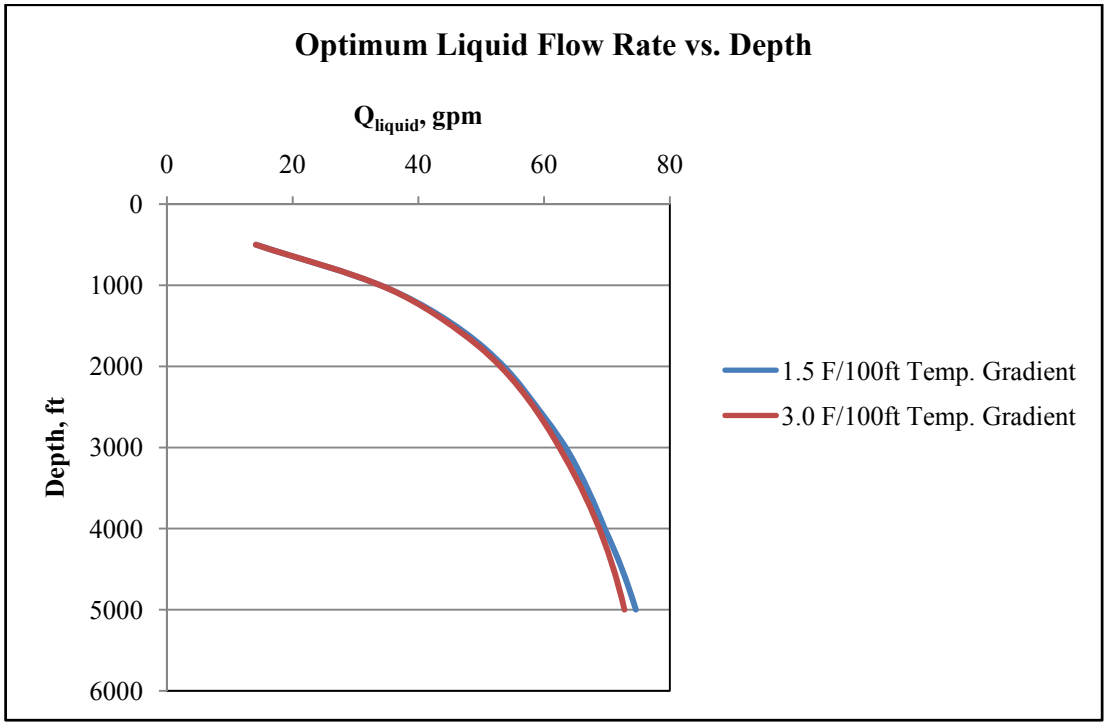

Figure 32 Change of Optimum Liquid Flow Rate with Depth and Temperature Gradient

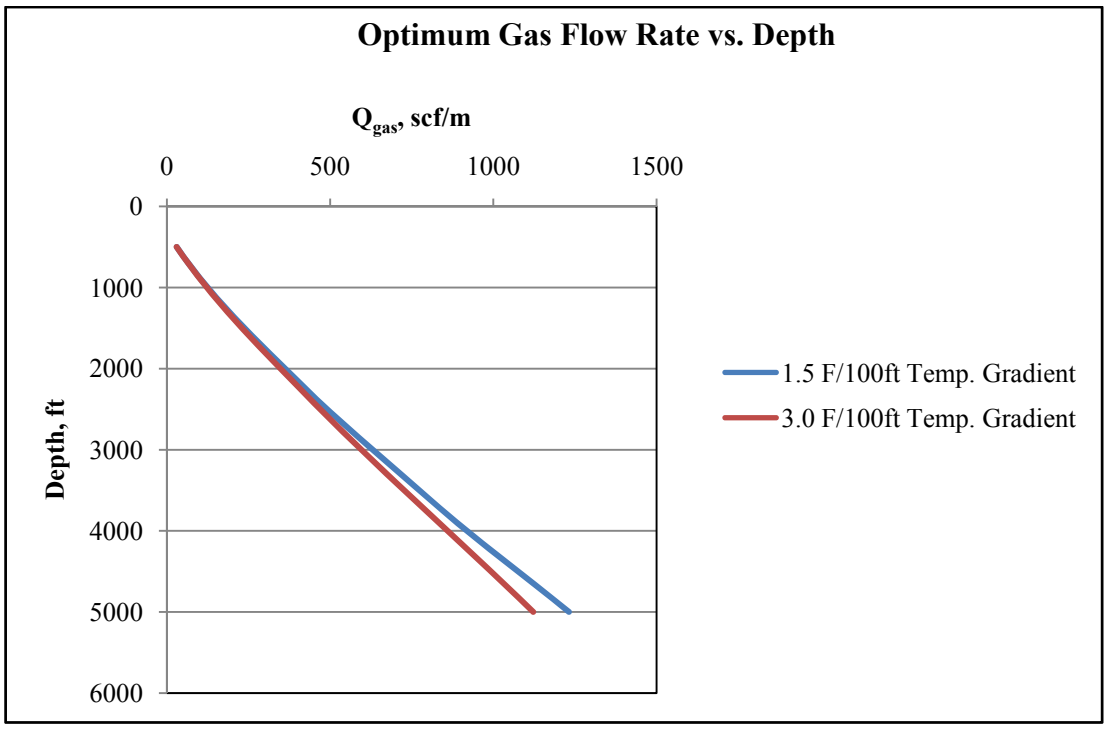

Figure 33 Change of Optimum Gas Flow Rate with Depth and Temperature Gradient

5.5. EFFECTS OF CHANGE IN NOZZLE SIZE

Figures 34 to 41 show the graphs for the output values of the model for $^{10}/_{32}$", $^{14}/_{32}$" and $^{18}/_{32}$" nozzle sizes versus depth with the 8 ½" hole size, 0.15 psi/ft pressure gradient and 1.5 ^{o}F/100ft temperature gradient.

The backpressure increases as the nozzle size increases (**Figure 34**). The calculation of the bit pressure drop involves division by the square of the total area of the bit nozzles. As the total area of three $^{10}/_{32}$" nozzles is smaller than three $^{14}/_{32}$" or three $^{18}/_{32}$" nozzles, rest staying same, the denominator is smaller and the bit pressure drop is higher (**Figure 35**). Since the major the pressure drop generally occurs at the bit considering the pressure losses in the circulating system, the pressure drop for the string (**Figure 36**) and the annulus (**Figure 37**) is expected to be the lowest for the $^{10}/_{32}$" nozzle size assuming the same inlet pressure.

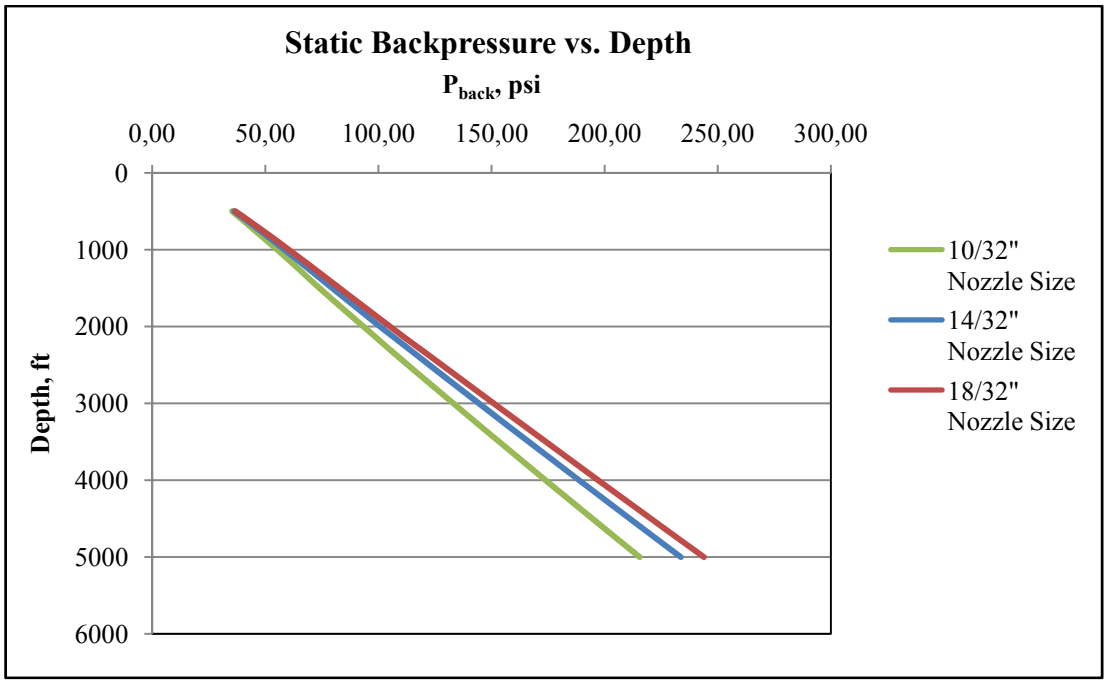

Figure 34 Change of Static Backpressure with Depth and Nozzle Size

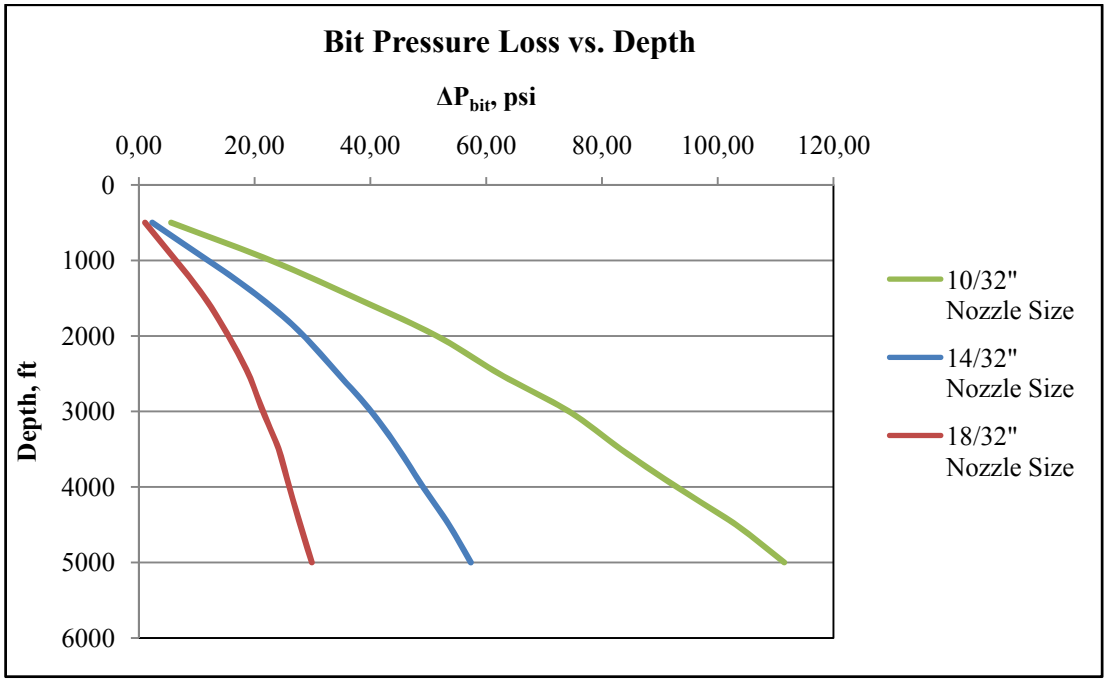

Figure 35 Change of Bit Pressure Loss with Depth and Nozzle Size

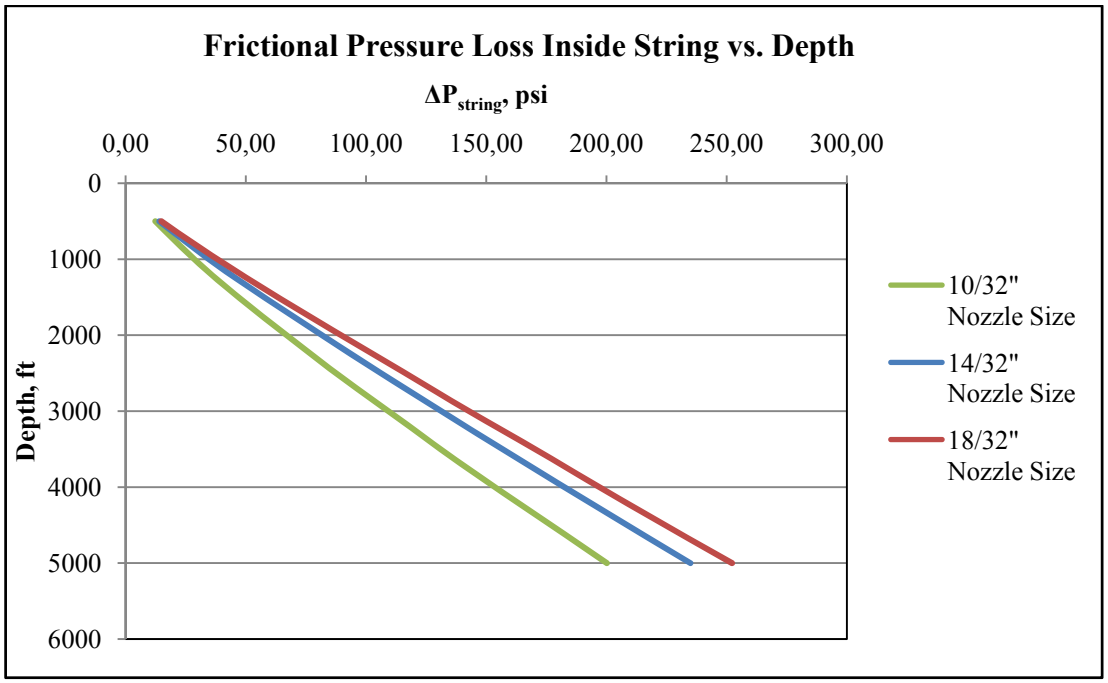

Figure 36 Change of Frictional Pressure Loss Inside String with Depth and Nozzle Size

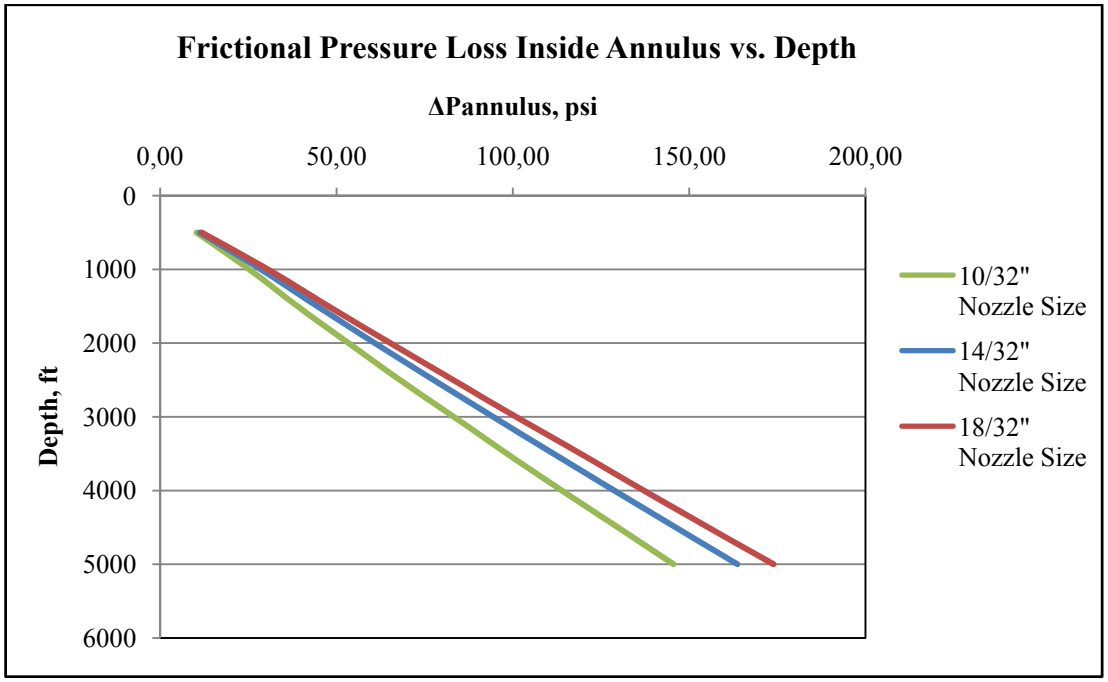

Figure 37 Change of Frictional Pressure Loss Inside Annulus with Depth and Nozzle Size

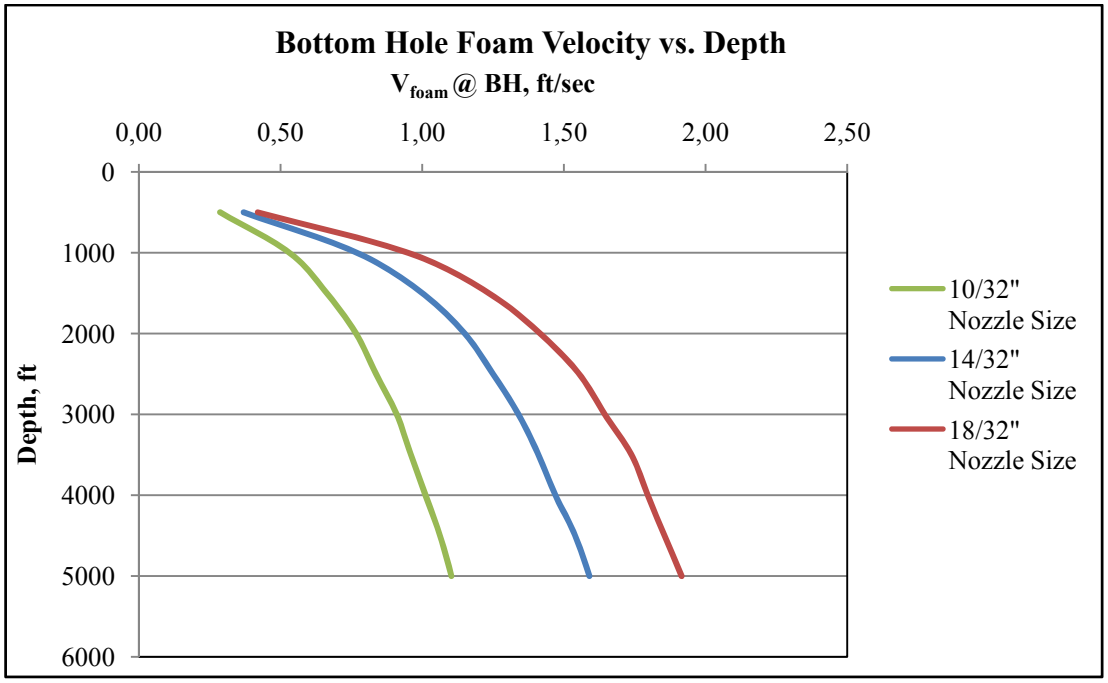

Figure 38 Change of Bottom Hole Foam Velocity with Depth and Nozzle Size

The bottom hole foam velocity increases with increased nozzle size (**Figure 38**). As the velocity is the flow rate per flow area and the flow rate is the mass rate divided by the density, rest staying constant, this change may be explained by the increase in the foam quality (**Figure39**), hence the decrease in the density.

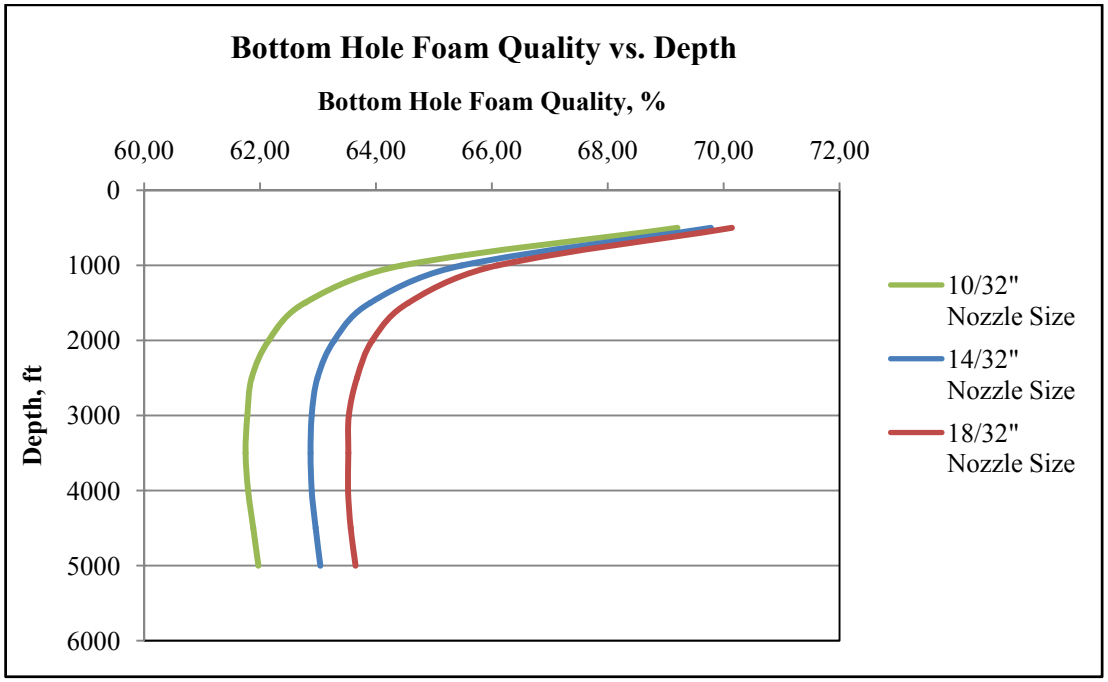

Figure 39 Change of Bottom Hole Foam Quality with Depth and Nozzle Size

The foam quality itself on the other hand is a function of the flow rates and the change in the foam quality is result of change in the optimum liquid flow rate (**Figure 40**) and the optimum gas flow rate (**Figure 41**) in order to meet the requirement of the maximum horsepower at the bit.

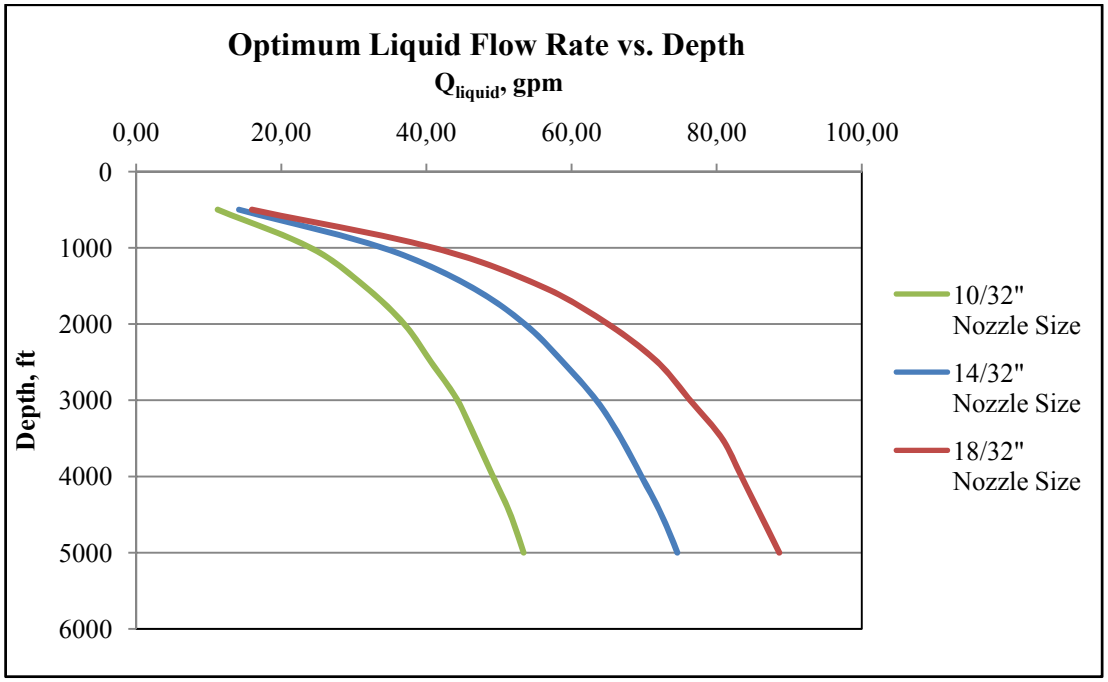

Figure 40 Change of Optimum Liquid Flow Rate with Depth and Nozzle Size

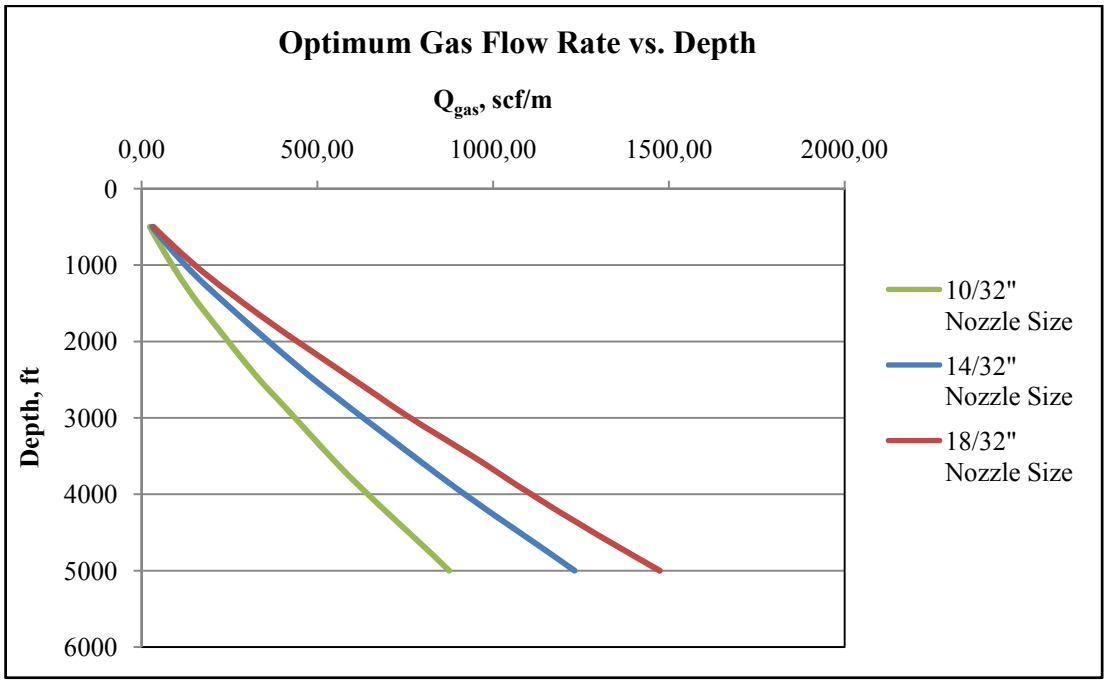

Figure 41 Change of Optimum Gas Flow Rate with Depth and Nozzle Size

5.6. OTHER RESULTS

This section identifies indirect findings from the model.

If all the pressure drops against depth are drawn on a graph (**Figure 42**) the trends agree with the expectations. The bit pressure drop is the highest, then the pressure drops inside the string and the pressure drops inside the annulus follow.

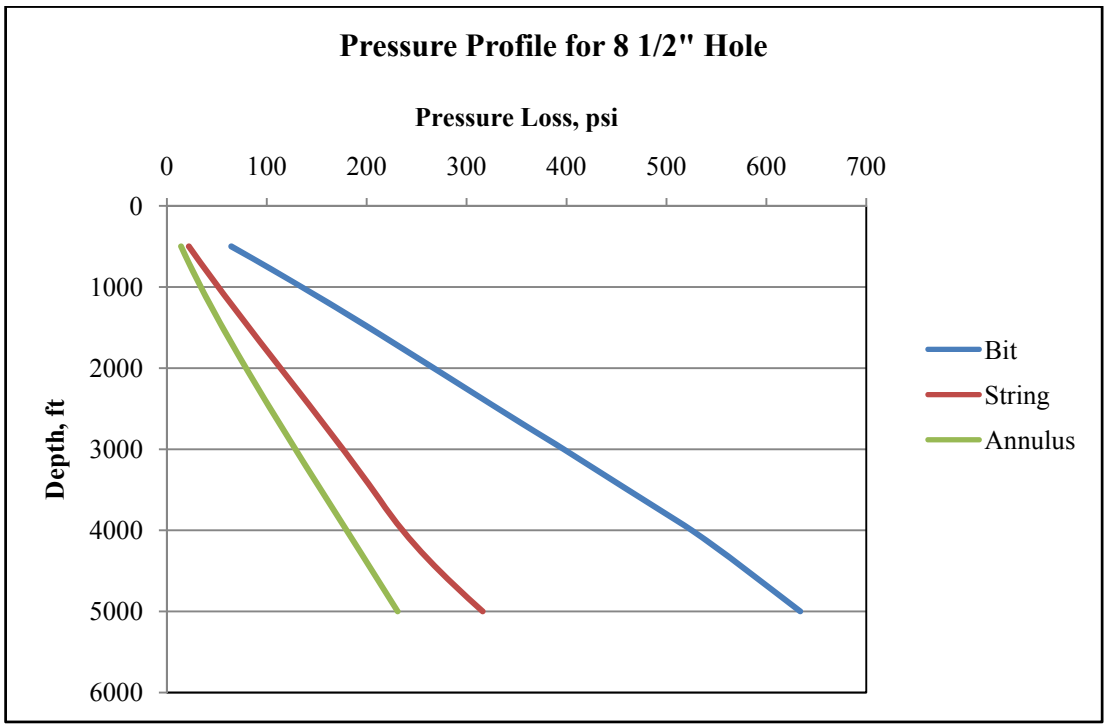

Figure 42 Pressure Drop Profile for 8 ½" Hole Size

Plotting the data points for optimum gas flow rate versus optimum liquid flow rates at the selected depths (**Figure 43**) show that for increasing hole size the optimum liquid flow rate and the optimum gas flow rate increases for a constant nozzle size. This is also in agreement with the decrease of the bottom hole foam quality with increasing hole size (**Figure 15**). This also means that rest staying constant the density of foam will increase with increasing hole size (**Figure 44**) since it is inversely proportional with the foam quality.

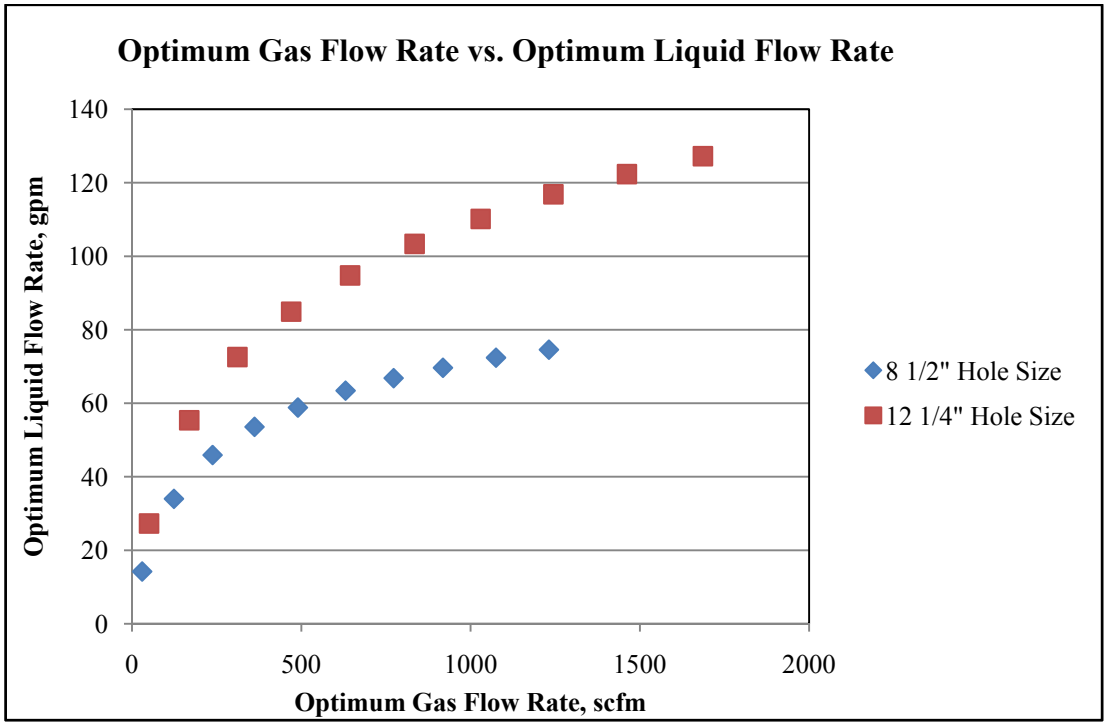

Figure 43 Plot of Optimum Gas Flow Rate versus Optimum Liquid Flow Rate for Selected Depths

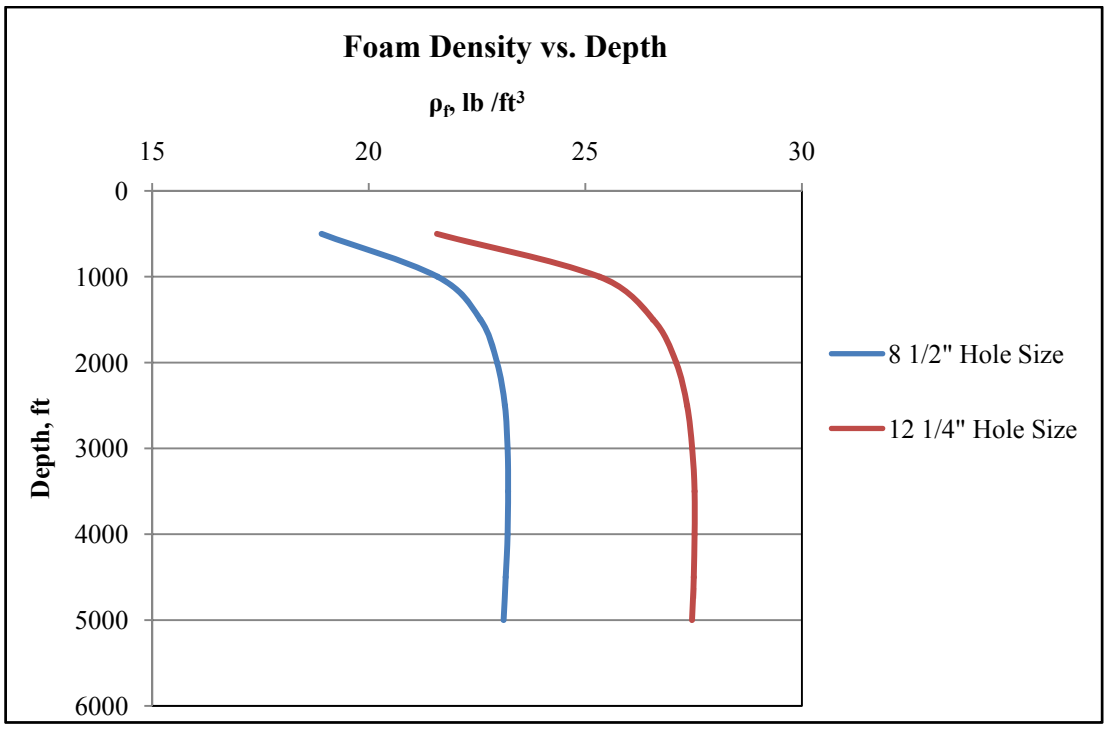

Figure 44 Change of Foam Density with Depth

Figure 45 shows the horsepower output at the bit. The horsepower is directly proportional with the flow rate. For a selected nozzle size the power output slightly increases with increasing hole size. This may be related to the change in the foam quality.

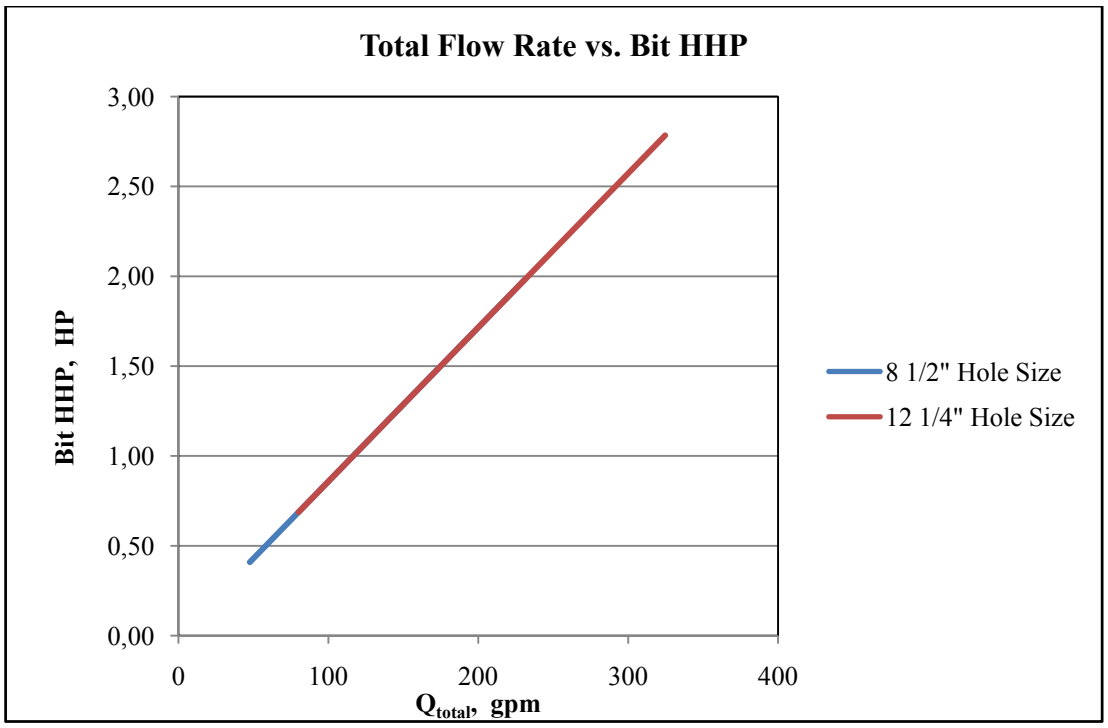

Figure 45 Change of Bit HHP with Total Flow Rate

Figure 46 presents the relation of the inlet pressure to the back pressure. It can be seen that there is a direct relation between the two. However, as hole size increases the backpressure decreases significantly.

Figure 47 is the graph of the relation of bottom hole foam velocity to the inlet pressure. For a constant inlet pressure when the nozzle size is increased, the bottom hole foam velocity also increases.

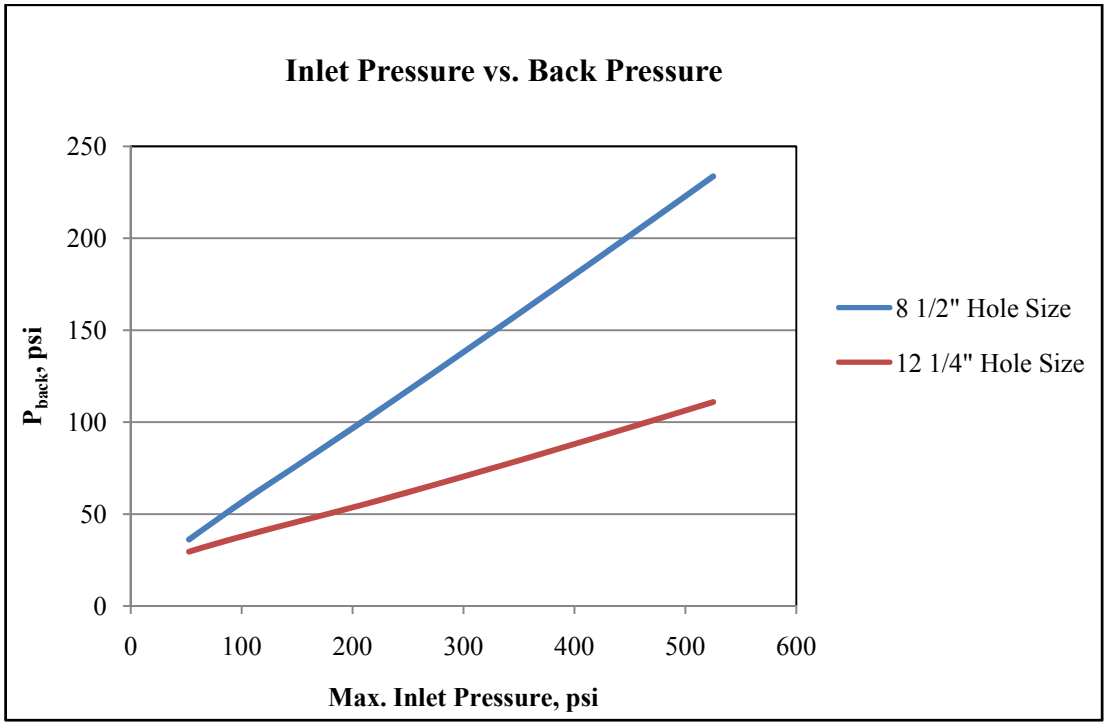

Figure 46 Inlet Pressure versus Back Pressure

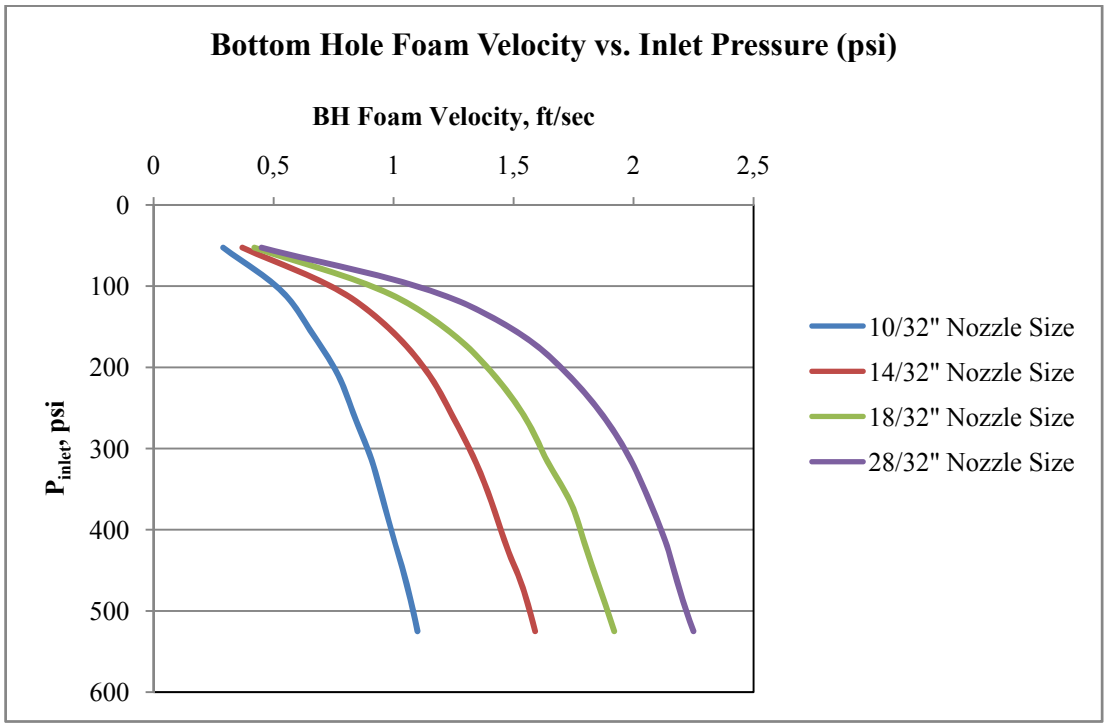

Figure 47 BH Foam Velocity vs. P_{inlet} for Varying Nozzle Sizes

CHAPTER 6

CONCLUSION

1. A new mathematical model was developed based on the mass flow rate of foam instead of volumetric flow rate. By this way compressibility of gas phase of foam was taken into account.

2. A computer code was developed based on the maximum bit hydraulic bit horsepower criteria at the bottom hole. It is processing the varying input data which are; drill pipe inner and outer diameters, hole size and depth of the well, inlet temperature and pressure of the foam into the system, temperature gradient of the formation and pressure at the final depth.

   After several iterations, pressure losses (pressure losses at the drill-string, bit and annulus) are obtained for varying nozzle sizes. Depending on pressure losses, optimum total flow area (nozzle size) can be chosen.

   Also, bottom hole foam quality, optimum static back pressure, gas and liquid flow rate values are acquired as program results.

3. Sensitivity analysis is performed for input parameters.

A) As hole size increases;
   Static back pressure applied should be decreases.
   Bit pressure loss and frictional pressure loss at the drill string increases.
   Bottom hole foam velocity and quality decreases.
   Optimum gas and liquid flow rates are increases as expected.

B) As pressure gradient of formation increases;
   Static back pressure applied should not affect slightly.
   Bit pressure loss and frictional pressure loss at the drill string increases.

Bottom hole foam velocity increases and quality decreases.
Optimum gas and liquid flow rates are increases.

C) As temperature gradient of formation increases;
Only bottom hole foam quality affected directly proportional with temperature. Changes for the other parameters can be neglected.

D) As nozzle size increases;
Static back pressure applied should be increases.
Bit pressure loss decreases and frictional pressure loss at the drill string increases.
Bottom hole foam velocity and quality increases.
Optimum gas and liquid flow rates are increases.

Moreover, the results from the computer program can be pasted to a spreadsheet and different tables or graphs can easily be generated by the user depending on his/her needs. Thus the program can be a valuable tool for field application where timely delivery of results is critical.

4. On the other hand when we compare the results with the other models, there is no one to one matching model existing. Godwin A.Okpobiri& Chi U.Ikoku has developed a model by neglecting pressure losses resulting from friction. They only considered frictional losses caused by solid phase. They have developed a model depending on particle settling velocities of solids. When their results are compared with proposed model, it is not slightly differing. But parameters depending on frictional losses are varying.

   Krug, J.A. and Mitchell, B.J presented charts for foam optimization considering; minimum annular return velocity, maximum foam quality, minimum required horsepower for injection. The optimization parameters are not same with the proposed model. But when we compare the results there is not too much gap between them.

E. Kuru O.M Oksenbur Model offers to determine optimum gas, liquid injection rates in vertical wells while keeping BHP at minimum. Also, for this model optimization parameters are not same with the proposed model.

CHAPTER 7

FUTURE RECCOMENDATIONS

The model is based on several assumptions such as vertical wellbore geometry, constant drillstring size and no influx. In order to develop the proposed model these assumptions may be eliminated and the model may be modified to include directional wellbore geometry, compartmentalized to introduce variable size drillstring and also arranged to include influx from the formation.

All the equations that were used to build up the model are accepted in the industry and the results from the model are always in the reasonable range. Still, even though it is not easy to find field records of foam drilling parameters open to public, it would also be ideal to compare the results of the model to field data if possible in order to build confidence to the proposed model.

REFERENCES

1. Moffitt, S., *Reed Tool Co. Data Book*, Houston, 1991.
2. Lorenz, H.,: "Field Experience Pins Down Uses for Air Drilling Fluids," *Oil and Gas J.* (May 12, 1980).
3. *Underbalanced Drilling Manual*, Gas Research Institute, Chicago, 1997.
4. Beyer, A.H., Millhone, R.S., and Foote, R.W.: "Flow Behavior of Foam as a Well Circulating Fluid," paper SPE 3986 presented at the 1972 SPE Annual Conference and Exhibition, San Antonio, Texas, 8-11 October.
5. Sibree, J.O.: "The Viscosity of Froth," *Faraday Soc. Trans.* (1934) **30**, 325.
6. Raza, S.H., and Marsden, S.S.: "The Streaming Potential and the Rheology of Foam," *SPE J.* (1967) **7**, 4.
7. David, A., and Marsden, S.S.: "The Rheology of Foam," paper SPE 2544 presented at the 1969 SPE Annual Meeting, Denver, 28-30 September.
8. Blauer, R.E., Mitchell, B.J., Kohlhaas, C.A.: "Determination of Laminar, Turbulent, and Transitional Foam Flow Losses in Pipes," paper SPE 4885 presented at the 1974 SPE Annual California regional Meeting, San Francisco, 4-5 April.
9. Lord, D.L.: "Mathematical Analysis of Dynamic and Static Foam Behavior," paper SPE 7927 presented at the 1979 SPE Symposium on Low Permeability Gas Reservoirs, Denver, 20-22 May.
10. Sanghani, V.: "Rheology of Foam and its Implications in Drilling and Cleanout Operations," M.S. thesis, U. of Tulsa, Tulsa, Oklahoma (1982).
11. Okpobiri, G.A., and Ikoku, C.U.: "Volumetric Requirements for Foam and Mist Drilling Operations," paper SPE 11723 presented at the 1983 SPE California Regional Meeting, Ventura, 23-25 March.
12. Sanghani V., and Ikoku C.U., .Rheology of Foam and Its Implications in Drilling and Cleanout Operations., Journal of Energy Resources Technology, Volume 105, pp.362-371 (September, 1983).
13. Reidenbach,V.G.,Harris, P.C., Lee, Y.N., and Lord, D.L.: "Rheology Study of Foam Fracturing Fluids Using Nitrogen and Carbon Dioxide," paper SPE

12026 presented at the 1983 Technical Conference and Exhibition, San Francisco, 5-8 October.

14. Spoerker, H.F., Trepess, P., Valko, P., Economides, M.J.: "System Design for the Measurement of Downhole Dynamic Rheology for Foam Fracturing Fluids," paper SPE 22840 presented at the 1991 SPE Technical Conference, Dallas, 6-9 November.
15. Guo, B., Miska, S., and Hareland, G.: "A Simple Approach to Determination of Bottom Hole Pressure in Directional Foam Drilling," *ASME Drilling Technology*, (January 1994).
16. Liu, G., and Meldy, G.H.: "Foam Computer Model Help in Analysis of Underbalanced Drilling", *Oil and Gas J.* (1996) **94**, No. 27, 114.
17. Gardiner, B.S., Dlugogorski, B.Z., and Jameson, G.J.: "Rheology of Fire Fighting Foams," *Fire Safety J.* (May 1998) 61-75.
18. Argillier J.F., Saintpere S., Herzhaft B., Toure A.,: "Stability and Flowing Properties of Aqueous Foams for Underbalanced Drilling,", paper SPE 48982 presented at the 1998 SPE Annual Technical Conference and Exhibition, New Orleans, 27-30 September.
19. Özbayoğlu, M.E., Kuru, E., Miska, S., and Takach, N.,: "A Comparative Study of Hydraulic Models for Foam Drilling," paper SPE 65489 presented at the 2000 Horizontal Well Technology Conference, Calgary, Alberta, Canada, 6-8 November.
20. Guo, B., Sun, K., and Ghalambor, A.,: "A Closed Form Hydraulics Equation for Predicting Bottomhole Pressure in UBD With Foam," paper SPE 81640 presented at the 2003 Underbalanced Technology Conference, Houston, 25-26 March.
21. Sun, K.,: "Pressure Requirements in Foam Drilling," paper AADE-03-NTCE-60 presented at the AADE 2003 National Technology Conference, Houston, 1-3 April.
22. Eren, T., "Foam Characterization: Bubble Size and Texture Effects," Master of Science Thesis, Middle East Technical University, 2004.
23. Kuru, E., Okunsebor, O.M., and Li, Y.,: "Hydraulic Optimization of Foam Drilling for Maximum Drilling Rate in Vertical Wells," paper SPE 91610

presented at the 2004 SPE/IADC Underbalanced Technology Conference and Exhibition, Houston, 11-12 October.

24. Doğan, H.A., Gücüyener, I.H., and Özbayoğlu, M.E., "A Comprehensive Bit Hydraulics Model for Gasified Drilling Fluids," paper SPE 99596 presented at the 2006 SPE/ICoTA Coiled Tubing and Well Intervention Conference, Woodlands, 4-5 April.
25. Einstein, A.,: "Eine neue Bestimmung der Molekuldimensionen," Annalen der Physic (1906) **19**, 289.
26. Hatschek, E.,: "Die Viskositat der Dispersoide. I. Suspensiode," Kalloid Z. (1910) **7**, 301.
27. Hatschek, E.,: "Die Viskositat der Dispersoide. II. Die Emulsionen," Kalloid Z. (1910) **8**, 34.
28. Mitchell, B.J.,: "Test Data Fill Theory Gap on Using Foam as a Drilling Fluid," *Oil and Gas J.* (September 6, 1971), 96.
29. Azar, J.J.: "Drilling in Petroleum Engineering," U. of Tulsa Press (1982), 256.
30. Vonthethoff, M.L., Schoemaker, S., and Telesford, A., "Underbalanced Drilling in a Highly Depleted Reservoir, Onshore South Australia," paper SPE 121632 presented at the 2009 SPE European Formation Damage Conference, Scheveningen, 27-29 May.
31. Krug, J.A. and Mitchell, B.J.,: "Charts Help Find Volume Pressure Needed for Foam Drilling," *Oil and Gas J.* (February 7, 1972), 61.

APPENDIX A

OPTIMIZATION PARAMETERS

Work by Jack A. KRUG and Dr. B.J. MITCHELL used parameters of;

Minimum annular return velocity
Maximum foam quality
Bottom hole pressure
Minimum required horsepower for injection

CONCLUSIONS OF THE STUDY WAS

1. Air and water volume rates for foam drilling operations can be specified.
2. Bottom hole pressures and injection pressures can be calculated.
3. Minimum hydraulic horse power for a foam drilling operation will occur when annulus back pressure is 14.7psia.
4. Any deviation from the specified minimum hydraulic horse power will require additional air volumes and injection pressure
5. As depth increases higher injection pressures and larger air and water volumes will be required.
6. Circulating bottom-hole pressure increases with depth and drilling rate.
7. Higher penetration rates will require an increase in the injection pressure and no practical change air in the injection air and water volumes.

CHARTS FROM Jack A. KRUG and Dr. B.J. MITCHELL

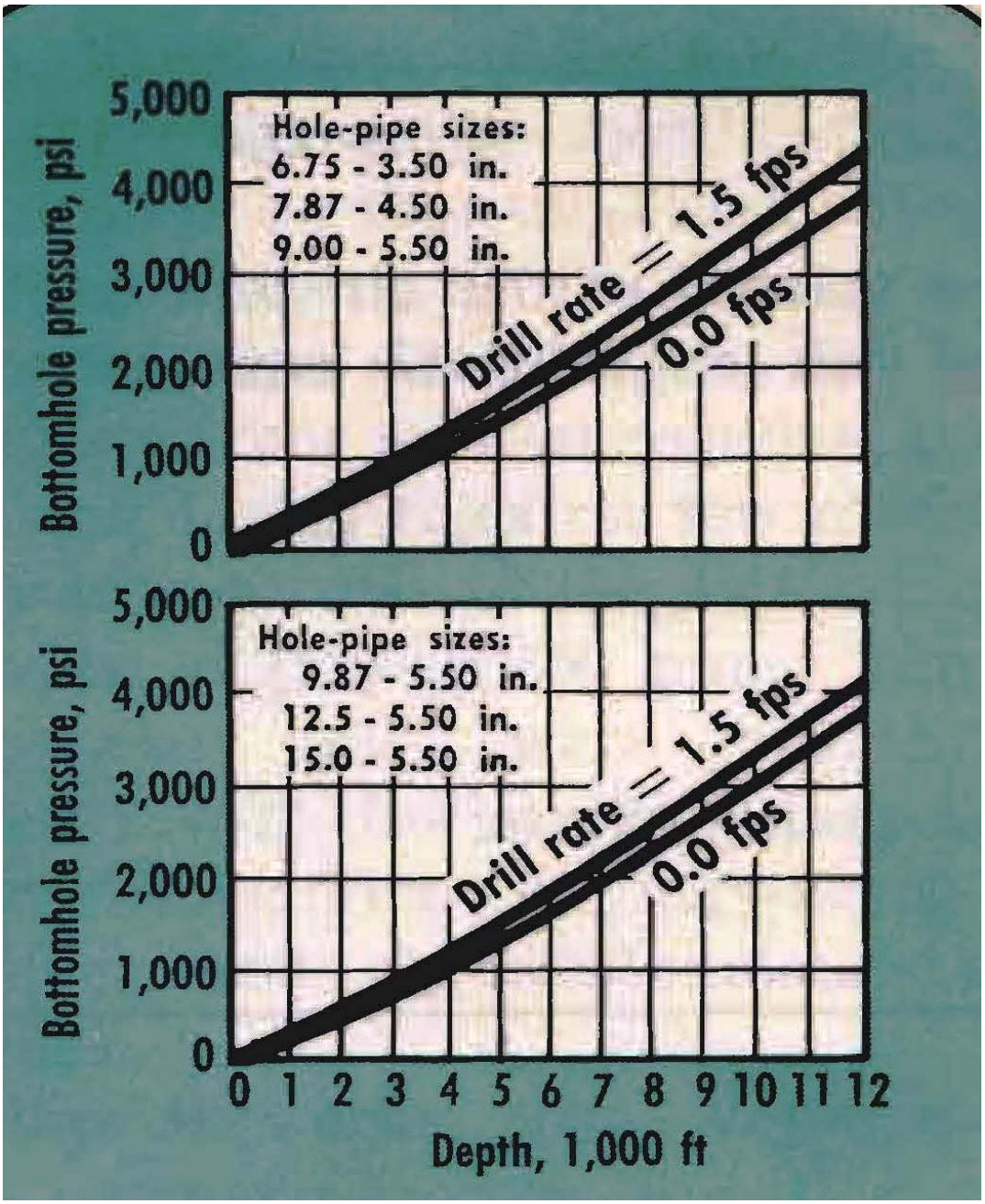

Figure A.1 Circulating Pressures

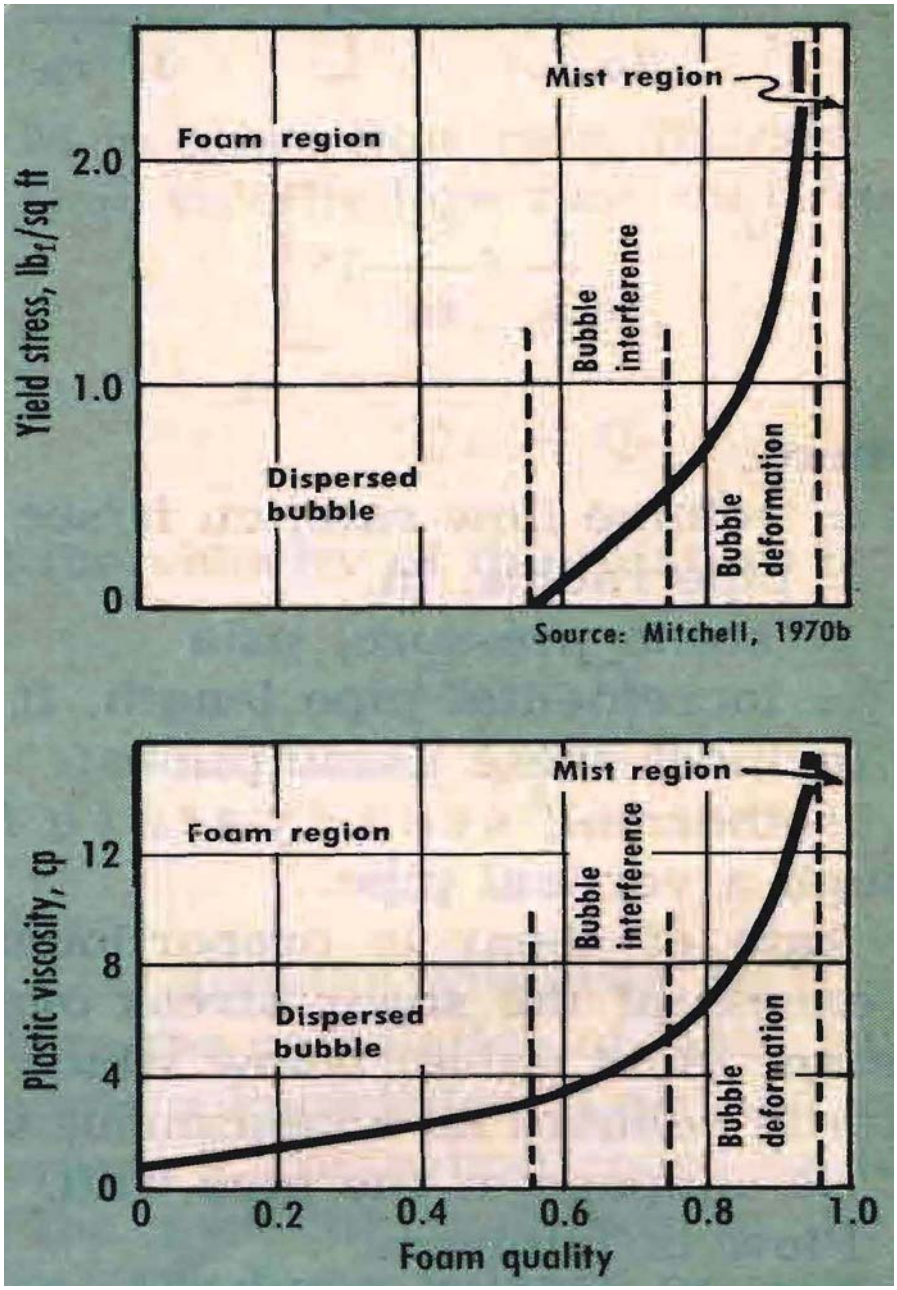

Figure A.2 Stress and Viscosity

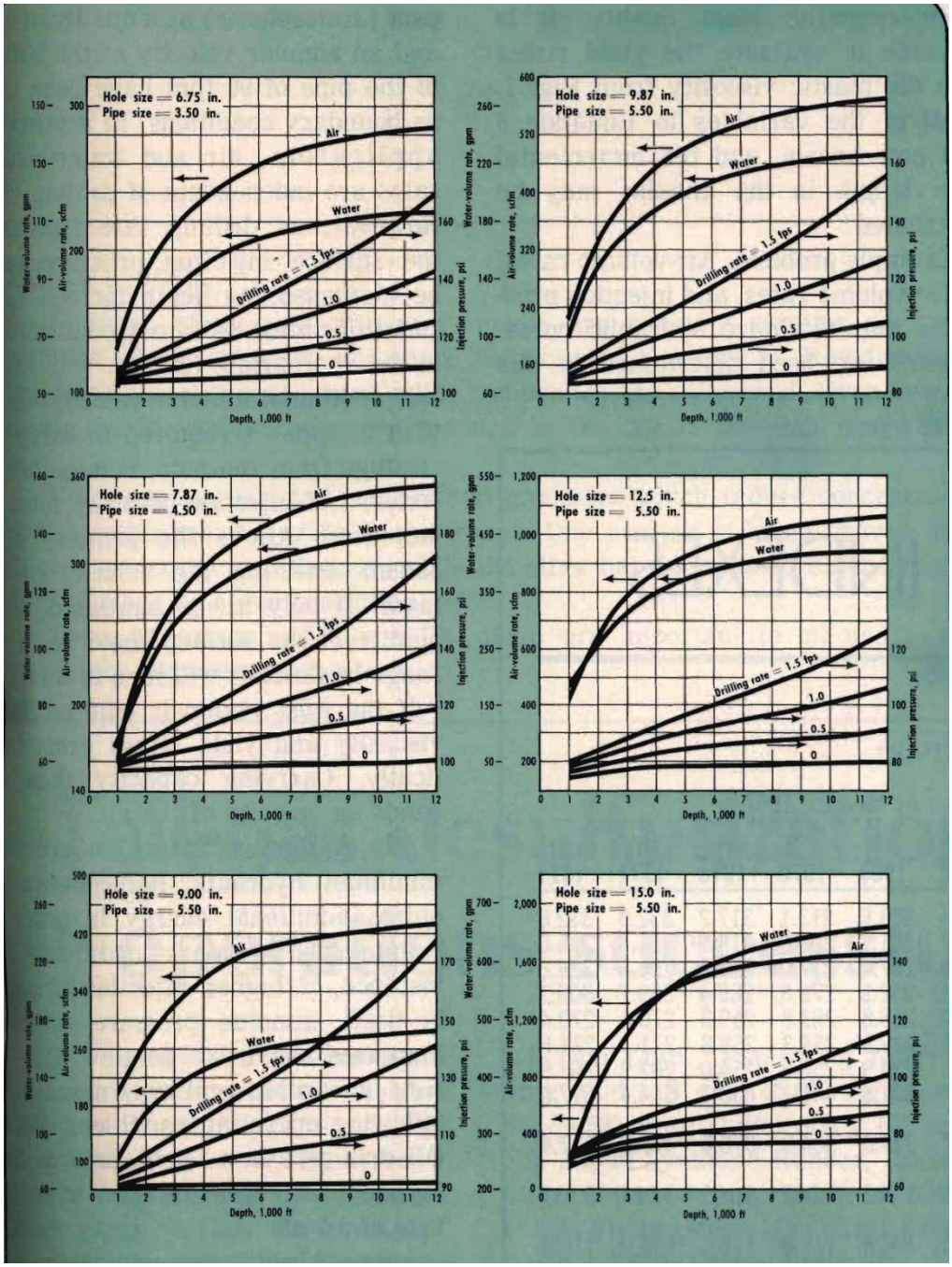

Figure A.3 Air and Water Requirement at Minimum Hydraulic HP

APPENDIX B

VOLUMETRIC REQUIREMENTS FOR FOAM AND MIST DRILLING OPERATIONS

Godwin A. Okpobiri and C.U. Ikoku formed a model that predicts pressure drop across bit nozzles for foam and mist is presented. It accounts for the compressibility of foam but assumes negligible pressure losses resulting from friction and change in elevation. It is developed for predicting minimum volumetric requirements for foam and mist drilling operations. it accounts for the frictional losses caused by the solid phase, pressure drop across bit nozzles, and particle-settling velocity. The technique offers a high degree of flexibility in the selection of wellhead injection pressures and volumetric injection rates.

Results indicate that volumetric requirements increase with increasing hole size, depth, and particle size. Increases in penetration rate cause only minor increases in volumetric requirements. Ali foam-drilling and well-cleanout operations can be accomplished within the laminar flow region with adherence to 0.55 minimum bottom hole and 0.96 maximum annular foam quality. Annular backpressures greater than atmospheric pressure are needed to maintain a bottom hole foam quality of 0.55 or more while reaching reasonable depths. To maintain constant depth as backpressure increases, however, both wellhead injection pressure and gas injection rate must be increased, and liquid flow rate decreased.

Minimum Volumetric Gas and Liquid Requirements:

Prediction of volumetric requirements and injection pressures necessitates an evaluation of the total system pressure drop that consists of pressure drop (1) inside the drill string or drill pipe, (2) across the bit, and (3) in the annular space. A set of drilling conditions should be known: annular backpressure, surface temperature, drill pipe diameter, hole size, bit nozzle size, geothermal gradient, foam quality at the top

of the annular space, fluid rheological properties, characteristics of the rock to be drilled, initial foam flow rate, desired penetration rate, and desired total well depth.

A computer program called GLVRFD has been written to perform the necessary predictions.

Results of this Model:

The foam drilling model (computer program GLVRFD) was used to simulate actual drilling conditions. The model, which is based on Ostwald-de Waele's power-law rheological model, involves a complete evaluation of the total system pressure drop. Pressure drop across bit nozzles, frictional losses caused by the solids phase and gas compressibility (deviation) factor are accounted for to present accurate predictions. The results show the certain relationships must be considered.

1. As depth increases, the liquid and air volume flow rates must be increased.
2. To maintain a bottom hole foam quality of 0.55 or more and to still reach reasonable depths, annular back-pressures greater than atmospheric pressure are required. For a constant depth as backpressure increases, however, both wellhead injection pressure and gas flow rate must be increased and liquid flow rate decreased.
3. As depth increases, injection pressure increases for a particular backpressure with increasing liquid and gas volume flow rates.
4. As the size of the particle to be lifted increases, volumetric requirements must also be increased.
5. Increases in penetration rate cause only minor increases in liquid and gas flow rates.
6. Pressure drop across me bit nozzles increases as cut-ting size increases.
7. For a constant particle size, pressure drop across the bit increases with hole size.
8. Pressure drop across the bit is virtually independent of penetration rate for a specific hole size and a constant cutting size.